Building Applied Photovoltaic Array:

Thermal Modeling and Fan Cooling

by

Jonathan Kyler Hrica

A Thesis Presented in Partial Fulfillment
of the Requirements for the Degree
Master of Science in Technology

Approved November 2010 by the
Graduate Supervisory Committee:

Govindasamy Tamizhmani, Chair
Bradley Rogers
Narciso Macia

ARIZONA STATE UNIVERSITY

December 2010

ABSTRACT

Thermal modeling and investigation into heat extraction methods for building-applied photovoltaic (BAPV) systems have become important for the industry in order to predict energy production and lower the cost per kilowatt-hour (kWh) of generating electricity from these types of systems. High operating temperatures have a direct impact on the performance of BAPV systems and can reduce power output by as much as 10 to 20%. The traditional method of minimizing the operating temperature of BAPV modules has been to include a suitable air gap for ventilation between the rooftop and the modules. There has been research done at Arizona State University (ASU) which investigates the optimum air gap spacing on sufficiently spaced (2-6 inch vertical; 2-inch lateral) modules of four columns. However, the thermal modeling of a large continuous array (with multiple modules of the same type and size and at the same air gap) had yet to be done at ASU prior to this project. In addition to the air gap effect analysis, the industry is exploring different ways of extracting the heat from PV modules including hybrid photovoltaic-thermal systems (PV/T).

The goal of this project was to develop a thermal model for a small residential BAPV array consisting of 12 identical polycrystalline silicon modules at an air gap of 2.5 inches from the rooftop. The thermal model coefficients are empirically derived from a simulated field test setup at ASU and are presented in this thesis. Additionally, this project investigates the effects of cooling the array with a 40-Watt exhaust fan. The fan had negligible effect on power output or

efficiency for this 2.5-inch air gap array, but provided slightly lower temperatures and better temperature uniformity across the array.

DEDICATION

To my Mother, Father, and Brother

ACKNOWLEDGMENTS

I would like to thank Dr. Govindasamy Tamizhmani for his continued support and guidance on this project. I would like to thank my committee members, Dr. Bradley Rogers and Dr. Narciso Macia, for their valuable feedback and review of this document. I would like to show appreciation to my colleagues at the Photovoltaic Reliability Laboratory at Arizona State University for their help and interest in the project. I would lastly, like to recognize the importance of the Photovoltaic Reliability Laboratory facility at Arizona State University in providing a great learning environment in which these types of experiments can be conducted.

TABLE OF CONTENTS

Page

LIST OF TABLES vii

LIST OF FIGURES viii

CHAPTER

1 INTRODUCTION 1

1.1 Background 1

1.2 Statement of Purpose 3

1.3 Scope 3

1.4 Assumptions 4

1.5 Limitations 4

2 LITERATURE REVIEW 6

2.1 Effect of Temperature on PV Cell Performance 6

2.2 Temperature Coefficients 7

2.3 Effect of Ambient Conditions of PV Module Temperature 9

2.4 Thermal Models 9

2.4.1 Nominal Operating Cell Temperature 9

2.4.2 Sandia Model 10

2.4.3 ASU-PTL Model 11

3 METHODOLOGY 13

3.1 Site Descripton 13

3.2 PV Array Installation 13

3.3 Programming of a CR1000 Datalogger 14

CHAPTER Page

3.4 Installation of Thermal Couples and Weather Instruments 18

3.5 Design and Construction of a Fan Cooling System 19

4 RESULTS & DISCUSSION 22

4.1 Air Gap Temperature 22

4.2 Effects of Wind Speed and Direction 24

4.3 Array Thermal Modeling for Temperature Prediction 25

4.4 Comparison of Coefficients between Two Studies 29

4.5 Fan Effect 32

4.5.1 Fan Effect Phase 1 Experiments – Thermal Modeling 32

4.5.2 Fan Effect on Array Temperature Uniformity 34

4.5.3 Fan Effect Phase 2 Experiments – Efficiency 37

5 CONCLUSIONS & RECOMENDATIONS 41

5.1 Conclusions 41

5.2 Recomendations 41

REFERENCES 42

APPENDIX

A LINEAR REGRESION PLOTS 43

LIST OF TABLES

Table Page

4.1 Summary of Derived Coefficients 27

4.2 Comparison of Coefficients between Two Studies 30

4.3 Measured Backsheet Temperature vs. Cell Temperature 31

4.4 Thermal Models for Fan in OFF and ON Positions..... 32

4.5 Predicted Array Average Temperature Using Derived Equations 33

4.6 Effect of Efficiency Gain (%) on Power Output..... 33

LIST OF FIGURES

Figure Page

2.1 Effect of Temperature on PV Cell Current and Voltage 6

2.2 Effect of Temperature on PV Cell Using Example Coefficients..... 8

3.1 Project Site and PV Array..... 14

3.2 CR1000 Enclosure and Weather Instruments 15

3.3 Wiring Schematic for CR1000 16

3.4 CR1000 Wiring Connections..... 17

3.5 Screenshot of PC200W Software Showing Real Time Data..... 18

3.6 Inline Duct Fan and Manifold..... 21

3.7 Array Ventilation System 21

4.1 Module & Air Gap Temperature July 15, 2010 23

4.2 Effects of Wind Speed and Direction on Array 24

4.3 Array Layout and Labeling..... 26

4.4 Module 1 Temperature °C Measured vs. Predicted Value 28

4.5 Array Average Temperature °C Measured vs. Predicted Value..... 29

4.6 Fan Effect on Array Temperature Uniformity 34

4.7 Array with Insulating Blocks on Sides..... 35

4.8 Fan Effect on Temperature Uniformity with Insulating Blocks..... 36

4.9 Top-Sub Array Efficiency with 15 min Fan ON/OFF..... 37

4.10 Middle-Sub Array Efficiency with 15 min Fan ON/OFF..... 38

4.11 Bottom-Sub Array Efficiency with 15 min Fan ON/OFF 38

4.12 Entire Array Efficiency with 15 min Fan ON/OFF 39

Chapter 1

INTRODUCTION

1.1 Background

There are many factors which can hinder the performance of building applied photovoltaic (BAPV) systems, but often the largest energy losses are due to the high operating temperatures of the photovoltaic (PV) modules. As the temperature of a PV module increases, the overall power output of the module can decrease by 0.5%/°C. A PV module can commonly reach temperatures of 45°C to 65°C during normal operation, which equates to a 10% to 20% loss of power as compared to the nameplate rating at 25^{o}C. During the summer months in Mesa, Arizona, BAPV modules can reach temperatures as high as 90°C depending on the air gap between module and rooftop. Thermal modeling and investigation into heat extraction methods for BAPV systems has become important for the industry in order to lower the cost per kilowatt-hour (kWh) of generating electricity from these types of systems.

Residential grid-tied BAPV systems have gained more attention in recent years as they are, in certain areas (with incentives), beginning to generate electricity at a price that is cost competitive. In an effort to continue with this trend, and create an even larger market for PV, industry professionals are continually looking for ways to lower the cost per kWh of PV systems. Many companies aim to lower manufacturing costs to achieve this, but improving system performance can be just as important. The cost per kWh of a PV system is calculated by dividing the total cost of the system by its estimated lifetime energy

production. Therefore, maximizing the amount of energy generated by a PV system will yield a lower cost per kWh. Increasing the daily output of a BAPV system can add up to a significant reduction in cost over a lifetime of 25 to 30 years. Additionally, reducing operating temperature should significantly increase the lifetime as described by the well known Arrhenius law (for the typical failure mechanisms such as metallic corrosion, the lifetime is expected to double for every 10^{o}C decrease in operating temperature).

The design and proper installation of a BAPV system is critical to optimizing performance. In climates like that of Arizona, finding a design which limits the negative effect caused by high operating temperature could greatly lower the cost per kWh of a system. The traditional method of minimizing the operating temperature of BAPV modules has been to include a suitable air gap for ventilation between the rooftop and the modules. There has been research done at Arizona State University (ASU) which investigates the optimum air gap spacing for sufficiently spaced (2-6 inch vertical; 2-inch lateral) modules of four columns. However, the thermal modeling of a large continuous array (with multiple modules of the same type and size and at the same air gap) had yet to be done at ASU prior to this project.

In addition to the air gap method, the industry is exploring different ways of extracting the heat from PV modules. One such concept is the hybrid photovoltaic-thermal (PV/T) system in which the PV modules are coupled with a heat extraction medium such as water. The heat that is extracted from the modules

can then be utilized for other applications (such as water or space heating) in a heat exchange process.

1.2 Statement of Purpose

The intent of this project was to develop a thermal model for a small residential BAPV array consisting of 12 identical polycrystalline modules at an air gap of 2.5 inches from the rooftop. Additionally, this project investigates the effects of cooling the array with an exhaust fan. The results of this project may apply to industry professionals who are seeking to improve photovoltaic performance by minimizing the installed operating temperature of rooftop modules.

1.3 Scope

This project included the following components:

- Finishing construction of a simulated residential rooftop at the Arizona State University Photovoltaic Reliability Laboratory (ASU-PRL).
- Installation of 12 polycrystalline PV modules at an air gap of 2.5 inches from the rooftop.
- Programming of a Campbell Scientific CR1000 data acquisition system with an AM16/32 Multiplexer.
- Installation of 25, type-K thermocouples for monitoring module and air gap temperature, as well as the fan exhaust temperature.
- Installation of a RM Young wind speed and direction sensor.

- Installation of a Vaisala WXT520 weather station to record wind speed, wind direction, ambient temperature, relative humidity, rainfall, and atmospheric pressure.
- Installation of an EKO MS-602 pyranometer and an EETS calibrated PV reference cell to monitor plane of array (POA) global irradiance.
- Development of a thermal model for each module in the array and the entire array.
- Design, construction, and installation of a fan cooling system.
- Several fan experiments with the fan in the on and off position at varying intervals. The fan effect on module power output was recorded using a Daystar Photovoltaic Curve Tracer.

1.4 Assumptions

This experiment uses thermocouples which are adhered to the backsheet of the PV modules using thermal tape. This measured backsheet temperature is assumed (and determined) to be about 1.5^{o}C lower than the cell temperature of the PV modules. In addition, several weather instruments were used in close proximity (within 5 to 10 meters) to the PV array. These instruments measured conditions such as irradiance, ambient temperature, wind speed, and wind direction. It is assumed that the weather conditions recorded by these instruments are equal to the conditions acting on the PV array.

1.5 Limitations

This experiment is limited to the study of one PV array at a fixed location and orientation. Thermal conditions may vary with differing locations and orientation

with regards to the sun's path. Additionally, the PV modules in this experiment were left in an open-circuit condition and no load was attached except for brief intervals when the power output was measured using a capacitive load PV curve tracer. The operating temperatures of modules under open-circuit condition may be slightly lower (about 2^{o}C) than under maximum power operating conditions.

Chapter 2

LITERATURE REVIEW

2.1 Effect of Temperature on PV Cell Performance

As the temperature of a PV cell increases, the power output decreases due to a change in the properties of the material in which the cell is made. Most solar cells are made of semiconductor materials which, when absorbing light, have the ability to move an electron from a low energy (bound) state to a higher energy (free) state. Once the electron is in the free state, it can move to an external circuit. The amount of energy required to move an electron from the bound state to the free state is called the band gap. The band gap varies from material to material and is also dependent on the temperature of the material. Increasing the temperature will decrease the band gap and increase the likelihood that an electron will move from the bound state to the free state [1]. This decrease in band gap leads to a slight increase in the short-circuit current of a PV cell, but a more significant decrease in the open circuit-voltage as shown in Figure 2.1. The combined result is an overall loss of power from the cell.

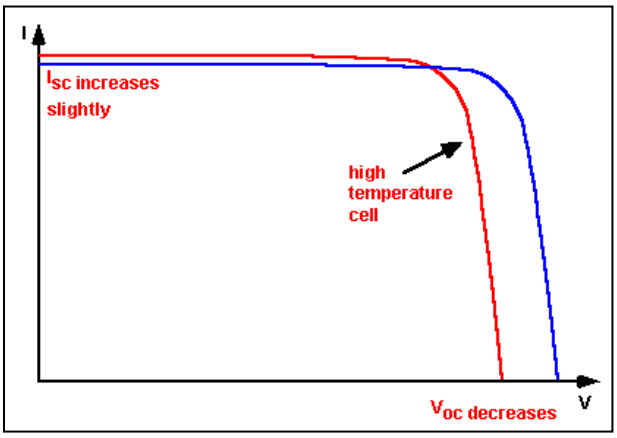

Figure 2.1 Effect of Temperature on PV Cell Current and Voltage [1]

2.2 Temperature Coefficients

Temperature coefficients are used to determine the effect of temperature on a PV cell in relation to the standard test condition (STC). The standard test condition was introduced as a way of normalizing power ratings of PV modules and is equal to an irradiance level of 1,000 W/m^2 at a cell temperature of 25°C. Testing modules under standard conditions allows for the comparison of the power rating of one module to another without having to factor in the effect of irradiance and temperature. However, these conditions are often not typical of real world operating conditions and may not give an accurate representation of how a module will perform in the field. It can be useful to know what effect the site-specific temperature will have on the performance of a module; therefore its effect is often calculated using temperature coefficients. The temperature coefficients for maximum power (P_{max}), open circuit voltage (V_{oc}), and short circuit current (I_{sc}) are usually listed in the manufactures specification sheet for each module. The coefficients represent a % change in P_{max}, V_{oc}, or I_{sc} for every °C the cell temperature differentiates from standard test conditions. The coefficient for P_{max} can be used in Equation (1) to determine the percent power change of a PV cell due to operating temperature [2].

$$\%\ Change\ Pmax = [(Tc - Tstc) * (Temp\ Coeff\ Pmax\ \%/°C)] \qquad (1)$$

Where:

Tc = Cell Operating Temperature (°C)

Tstc = Standard Test Conditions Temperature (25°C)

Similar equations can be used to determine the % change in V_{oc} and I_{sc} of a module at operating temperature. A plot of the effect of temperature on I_{sc}, V_{oc}, and P_{max} is shown in Figure 2.2 using example coefficients. Each module has its own specific coefficients based on the properties of the materials in which it is made, but are generally similar to the coefficients given in this example.

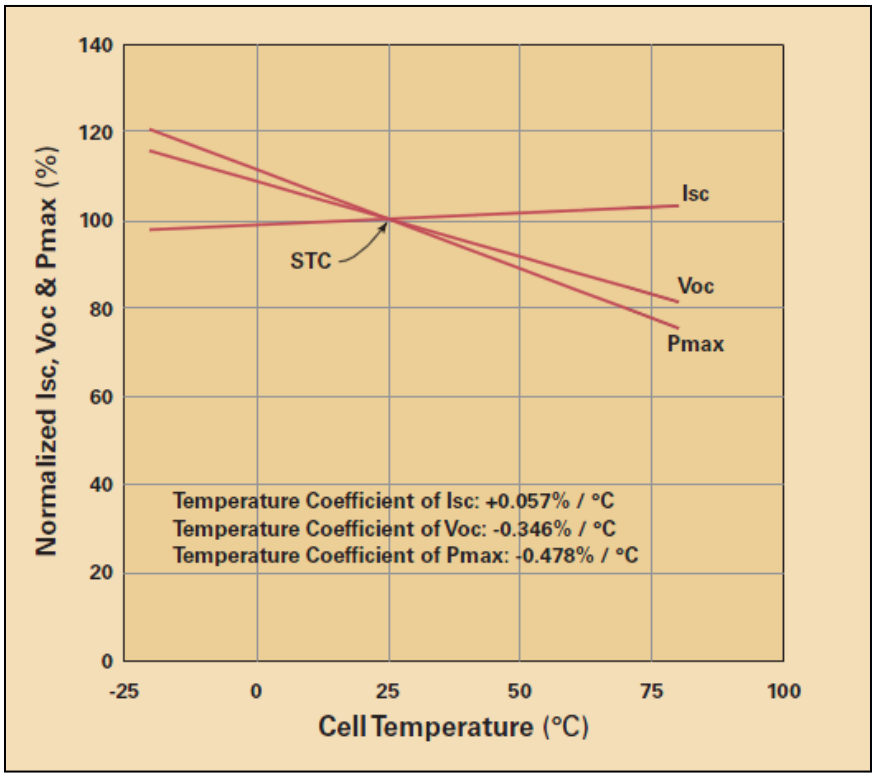

Figure 2.2 Effect of Temperature on PV Cell Using Example Coefficients [2]

As the cell temperature rises in Figure 2.2, the V_{oc} and fill factor decrease while the I_{sc} slightly increases. The overall result is a decrease in P_{max} with an increase in temperature. Since STC conditions also include an irradiance of 1000 W/m^2, this plot shows that the ideal operating conditions for a PV cell is at high irradiance with low temperature.

2.3 Effect of Ambient Conditions on PV Module Temperature

The first two sections of this chapter have shown that PV cell performance is influenced by operating temperature, but there are multiple factors which can determine operating temperature of BAPV modules. These factors include the ambient temperature, irradiance level, wind speed, wind direction, humidity, and proximity to the rooftop. Several thermal models have been developed in order to predict the temperature of a module at a given site with given ambient conditions.

2.4 Thermal Models

2.4.1 Nominal Operating Cell Temperature

The nominal operating cell temperature (NOCT) is the predicted temperature of the module under the ambient conditions of 800 W/m^2 in an ambient temperature of 20°C, and a wind speed of less than 1 m/s. The NOCT model provides a good estimate of the module temperature in various irradiance levels and ambient temperature conditions using a modules rated NOCT value with Equation (2) [3]:

$$T_c = T_A + \left(\frac{NOCT-20}{0.8}\right) G \quad (2)$$

Where:

T_c = Predicted Cell Temperature (°C)

T_A = Ambient Temperature (°C)

NOCT = Module NOCT value (°C)

G = Irradiance (kW/m^2)

The NOCT value will vary slightly from one module to another due to differences in construction and materials used. Manufacturers will often give the NOCT value

for each module on the module specification sheet so that customers can get a better estimation of what the power losses will be due to temperature.

2.4.2 Sandia Model

A simple thermal model for PV performance modeling purposes was developed at Sandia National Laboratories. The model is based on field experiments and is described in Equation (3) [4]:

$$T_m = E * (e^{a+b*WS}) + T_a \quad (3)$$

Where:

T_m = Back-surface module temperature, (°C).

T_a = Ambient air temperature, (°C)

E = Solar irradiance incident on module surface, (W/m^2)

WS = Wind speed measured at standard 10-m height, (m/s)

a = Empirically-determined coefficient establishing the upper limit for module temperature at low wind speeds and high solar irradiance

b = Empirically-determined coefficient establishing the rate at which module temperature drops as wind speed increases

The coefficients which are used in the Sandia model are determined by collecting thousands of temperature measurements recorded over several days. The data must be collected on clear days with no cloud cover or other temperature influencing transients. The model has been used in system design and has a proven accuracy of about ± 5°C [4].

2.4.3 ASU-PTL Model

A thermal model which predicts module temperature as a function of global irradiance, ambient temperature, relative humidity, wind speed, and wind direction was developed with parallel work done at ASU-PTL in Mesa, AZ and NREL in Golden, Colorado. Temperature data was collected on multiple modules at both sites for a period of two years from 2000 to 2002. In addition, the ambient weather conditions were recorded. A neural network program was used to analyze the data and the coefficients for Equation (4) were developed [5]:

$$T_{module} = w1 * T_{ambient} + w2 * Irradiance + w3 * WindSpd + w4 * WindDir + w5 * Humidity + const \quad (4)$$

Where:

w1, w2, w3, w4, w5, const = empirically derived coefficients

T_{module} = Predicted Module Temperature (°C)

$T_{ambient}$ = Ambient Temperature (°C)

Irradiance (W/m^2)

Wind Speed (m/s)

This equation was then compared to a second equation that had only three input parameters rather than five. The three input parameters were irradiance, ambient temperature, and wind speed described by Equation (5) [5]:

$$T_{module} = w1 * T_{ambient} + w2 * Irradiance + w3 * WindSpd + const \quad (5)$$

A regression analysis of both equations revealed that the three parameter equation was the stronger equation. Wind direction and humidity were found to have negligible effect on the module temperature, and the possible measurement error

in recording these values could lead to more deviation in the coefficients than the values themselves [5]. This three parameter model was developed using open rack PV modules and was included in an ASU master student thesis titled *Outdoor Energy Rating Measurements of Photovoltaic Modules* by Yingtang Tang [6].

The three parameter model was later applied to BAPV modules at various air gaps and evaluated in an ASU master student thesis titled *Temperature of Rooftop PV Modules: Effect of Air Gap and Ambient Condition* by Bijay Lal Shrestha [7]. A long term study of this model for BAPV modules at various air gaps was evaluated in an ASU master student thesis titled *Building Applied and Back Insulated Photovoltaic Modules: Thermal Models* by Jaewon Oh [8].

Lastly, this report applies the three parameter thermal model to a large continuous BAPV array with multiple modules of the same type.

Chapter 3

METHODOLOGY

3.1 Site Description

This project was conducted on a mock residential rooftop at Arizona State University's Photovoltaic Laboratory in Mesa, Arizona. The structure was built for the purpose of simulating a typical residential roof and is made of a wooden frame and other materials which are commonly used in residential construction. It is south facing, measures 19 feet by 17.5 feet, and is angled at a pitch of 23° from horizontal axis. At the project's beginning, the majority of the structure was in place, but the outer weatherproofing layer and shingles were missing. A layer of roofing felt and a layer of concrete tiles commonly used in residential applications were added to finalize the roof construction.

3.2 PV Array Installation

The installed array consists of (12) Polycrystalline Silicon modules at an air gap spacing (from module frame) of 2.5 inches from the roof as shown in Figure 3.1. The modules were aligned in 3 horizontal rows consisting of 4 modules each. The spacing between the rows is 1 inch and the spacing between the columns is 1/8 inch. Each row of modules was attached to two rails of Unistrut metal framing. The metal framing was then locked into the roof supports using 8 inch long by 3/8 inch diameter hex bolts.

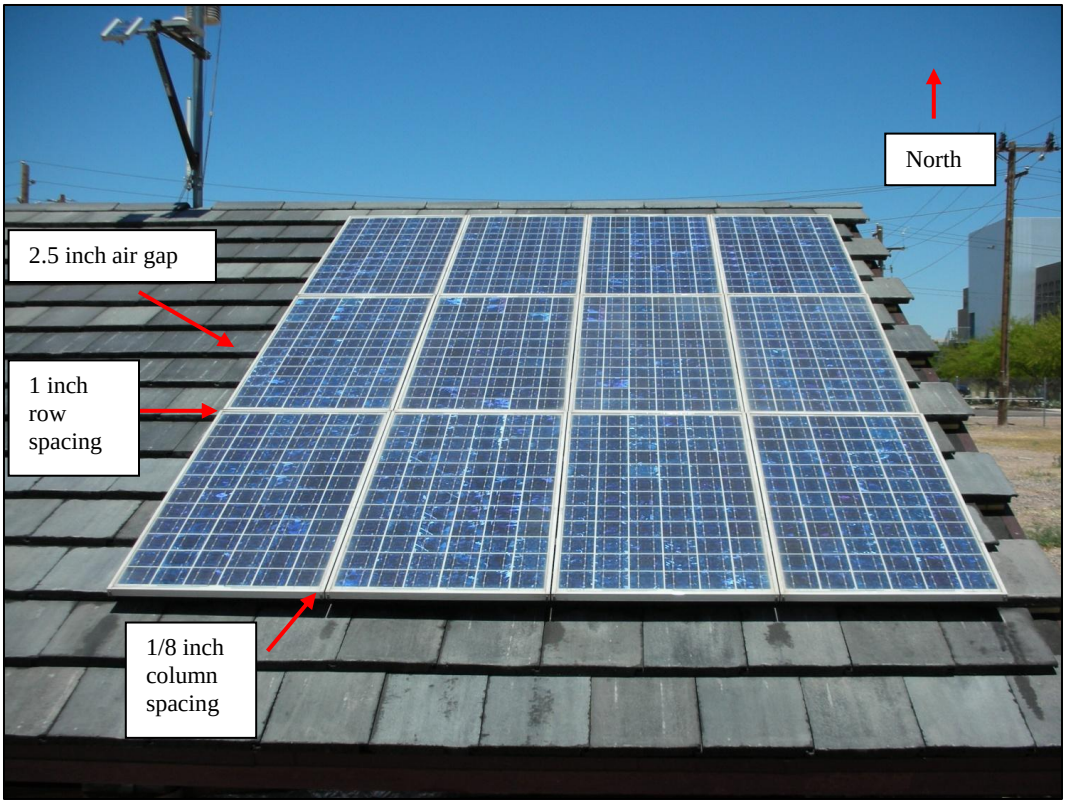

Figure 3.1 Project Site and PV Array

3.3 Programming of a CR1000 Datalogger

A Campbell Scientific CR1000 Datalogger was used in conjunction with an AM16/32 Multiplexer for the measurement and storage data from multiple sources. The instrumentation used in this project included twenty-five type-K thermocouples, a RM Young Wind Speed and Direction sensor, a Vaisala WXT520 Weather Station, an EKO MS-602 pyranometer and an EETS calibrated PV reference cell. The CR1000 was required to measure and store information from each of these devises on regular intervals. However, since the CR1000 only has 16 analog channels, the AM16/32 Multiplexer was used as an expansion device to allow for more sensor inputs.

The CR1000 and AM16/32 Multiplexer were housed in a ruggedized outdoor enclosure and mounted on the north side of the simulated rooftop structure as shown in Figure 3.2. An AC to DC rectifier was used in conjunction with a nearby 120 Volt AC outlet to provide the necessary 12 Volt DC power to the CR1000. Additional wiring provided power and communication to the AM16/32 Multiplexer.

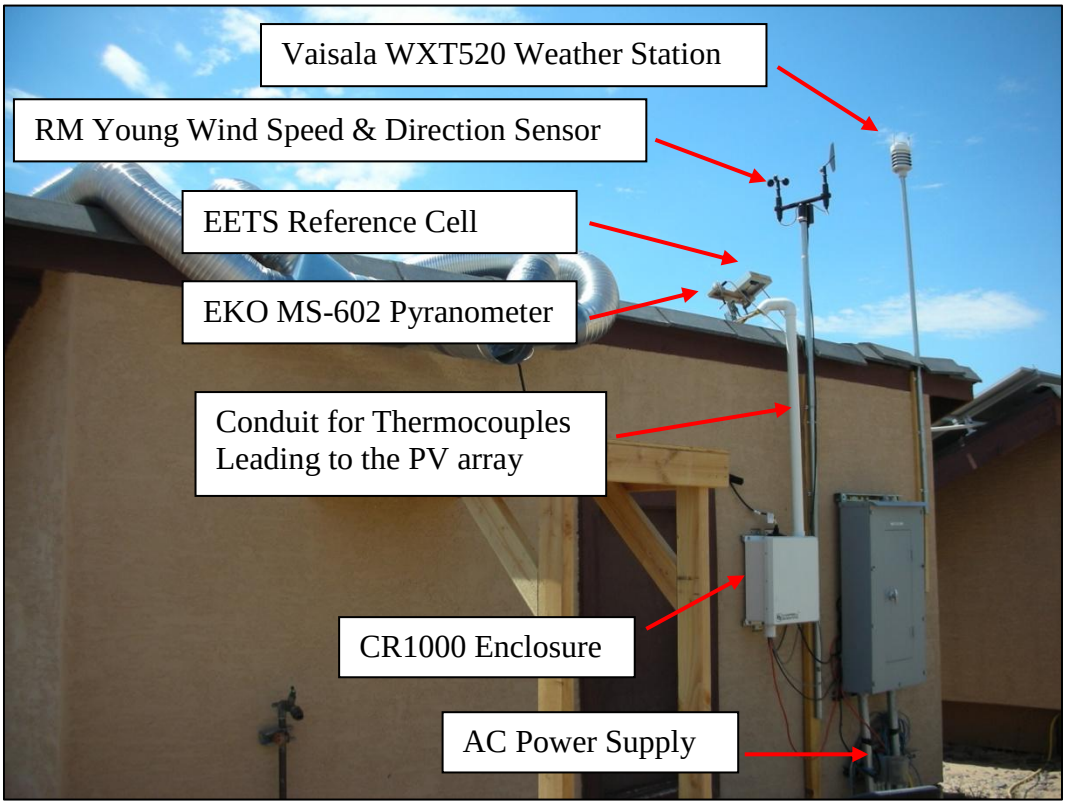

Figure 3.2 CR1000 Enclosure and Weather Instruments

The CR1000 has a basic operating system and it can be programmed to accommodate a wide range of instruments. The programs which run on the CR1000 operating system are coded in a computer language called CR Basic. Campbell Scientific has a Windows based computer program called Short Cut which creates individually tailored programs for the CR1000 operating system.

The programs created in Short Cut are designed to tell the CR1000 what instruments are connected to it, and how often to collect data from each instrument. The Short Cut program also develops wiring schematics for connecting various instruments to the CR1000 since the wiring is dependent on the programming. A portion of the wiring schematic for this project's setup is shown in Figure 3.3.

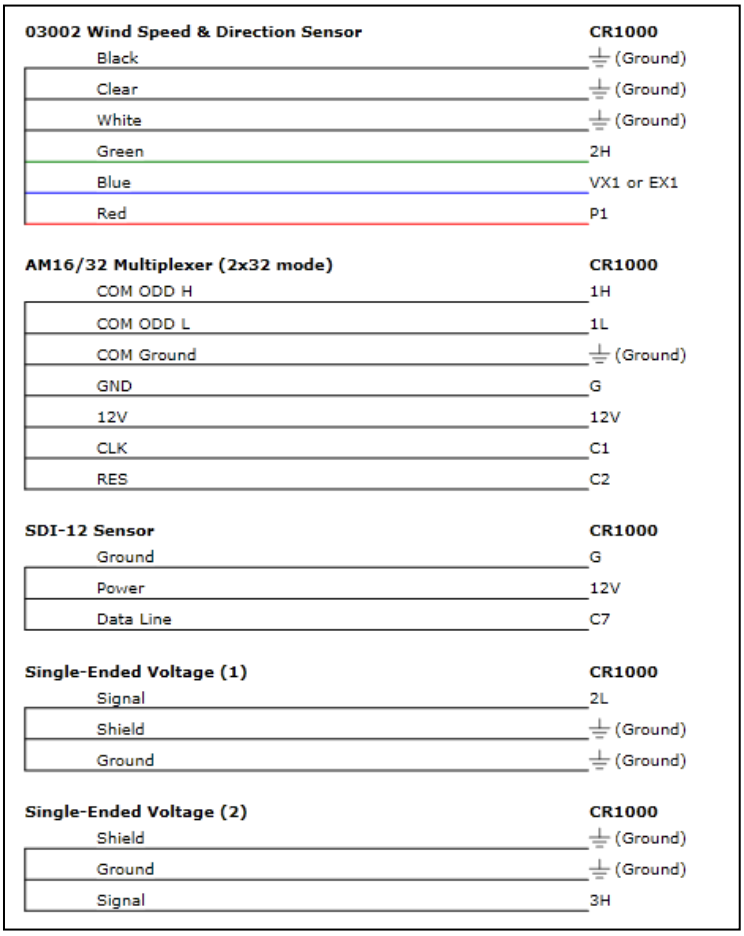

Figure 3.3 Wiring Schematic for CR1000

The wiring schematic shown in Figure 3.3 is based on a CR1000 program created using Short Cut and shows the wiring connection from each instrument to the CR1000 channels. A photograph of inside the CR1000 enclosure after all the connections had been made is shown in Figure 3.4

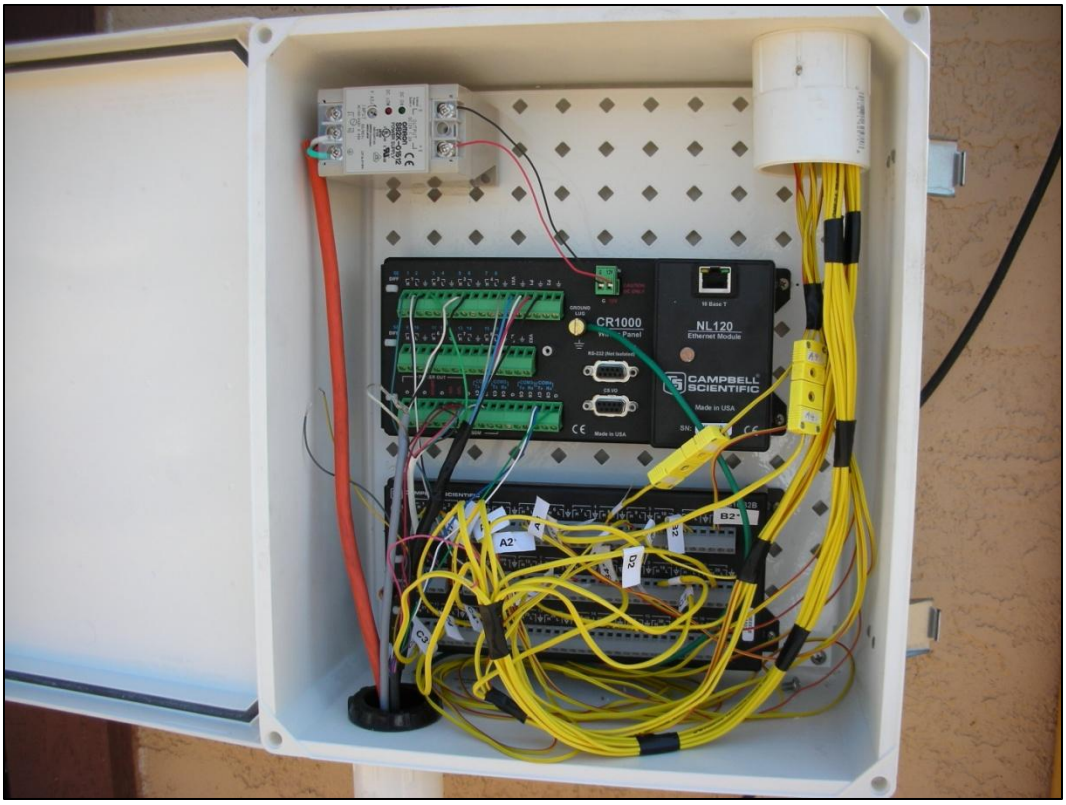

Figure 3.4 CR1000 Wiring Connections

The program which was created for this project was designed to tell the CR1000 to collect data from every sensor every minute. These values are then averaged together every 6 minutes, and saved in a table in the CR1000's memory. This table is then downloaded to a laptop computer using another Campbell Scientific program called PC200W. The CR1000 has an internal clock, which can be synchronized with a laptop computer using the PC200W program. The program ensures that data is collected on intervals that coincide with the end of every hour. For example, the averaged data is saved to the table exactly on the hour, then again exactly 6 minutes after the hour, and so on.

The PC200W software requires a RS-232 cable connection to communicate with the CR1000. Once the connection is made, the data coming

from the instruments can be monitored in real time, and all the historical data can be downloaded into a text file. The text file is then imported into Microsoft Excel for further analysis. The PC200W program also allows for adjustments of other functions of the CR1000 such as uploading or downloading programs, and synchronizing the internal clock with the connected laptop PC. A screenshot of the PC200W program monitoring real time data is shown in Figure 3.5.

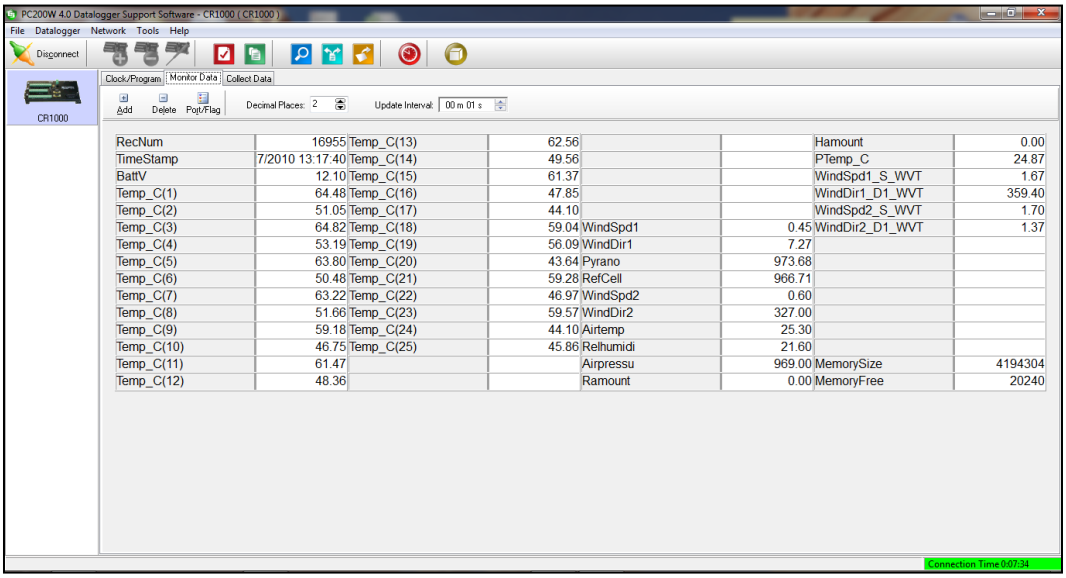

Figure 3.5 Screenshot of PC200W Software Showing Real Time Data

3.4 Installation of Thermocouples and Weather Instruments

A type-K thermocouple was attached to the backsheet of each module in the array using thermal tape. The tips of the thermocouples were in direct contact with the backsheet material and it was assumed that this temperature was equivalent to the cell temperature (in reality, the cell temperature is about 1.5^{o}C higher than the backsheet temperature). An additional thermocouple was also attached to the back of each module, but the tip of the thermocouple was left at a

distance of 1 inch from the backsheet. These thermocouples were used for collecting the air gap temperature data.

An EKO MS-602 pyranometer and an EETS calibrated PV reference cell were also installed on the rooftop co-planar to the array. These instruments were used to gather the plane of array (POA) irradiance levels. The EKO MS-602 was used as the primary collection device and the EETS reference cell was used as a backup to ensure that accurate readings were being recorded.

A RM Young Wind Speed and Direction sensor and a Vaisala WXT520 Weather Station were installed using suitable poles which were mounted to the north side of the rooftop structure with metal brackets. Both devises have wind speed and direction measuring capability, however the RM Young devise was used as the primary measuring device for wind speed and direction measurements. The Vaisala WXT 520 also has ambient temperature, relative humidity, atmospheric pressure, and rainfall measuring capability. The Vaisala WXT 520 was the primary device used for ambient temperature measurements.

Each of the instruments listed in this section were connected to the CR1000 Datalogger as described in Section 3.3 and data was collected according to the programming.

3.5 Design and Construction of a Fan Cooling System

The objective of this section of the project was to determine the feasibility of a ventilation system which would create significant air flow to cool the modules and overcome losses associated with high operating temperatures. This was done by constructing a low cost prototype using widely available components

found at a local hardware store. This method is sometime referred to as a "proof of concept" experiment and is used in applied research to establish feasibility and address technical issues.

The design started by determining the size of the fan which should be used. Since the friction losses associated with the air moving in-between the roof and the module were unknown, and difficult to estimate, the fan size was based on power rating rather than air flow calculations. The PV array in this experiment was rated for 1200 watts, under standard test conditions, and typical power losses of 10% to 20% due to high operating temperatures would equate to a 120 to 240 Watt loss of power for this array. Therefore, the maximum power consumption of the fan needed to be less than 120 Watts. Any fan with a higher power rating would consume more power than it is trying to accommodate for.

One of the original ideas was to use a DC fan which would be directly powered by the array, but due to the high cost and low availability of DC fans, an AC fan was selected instead and it was powered by an external source. The fan which was selected was a 40 Watt, 210 CFM, in-line duct fan. A fan of this type is primarily used as booster fan for residential HVAC systems and is able to operate at high temperatures. The fan was housed within 8 inch diameter circular ducting made of aluminum. The fan assembly was then attached to multiple 6 inch diameter aluminum ducts that act as a manifold to draw air from the top of the array as shown in Figure 3.6 and Figure 3.7. The fan essentially acts as an exhaust to the top of the array, aiding air flow from the bottom to the top of the array.

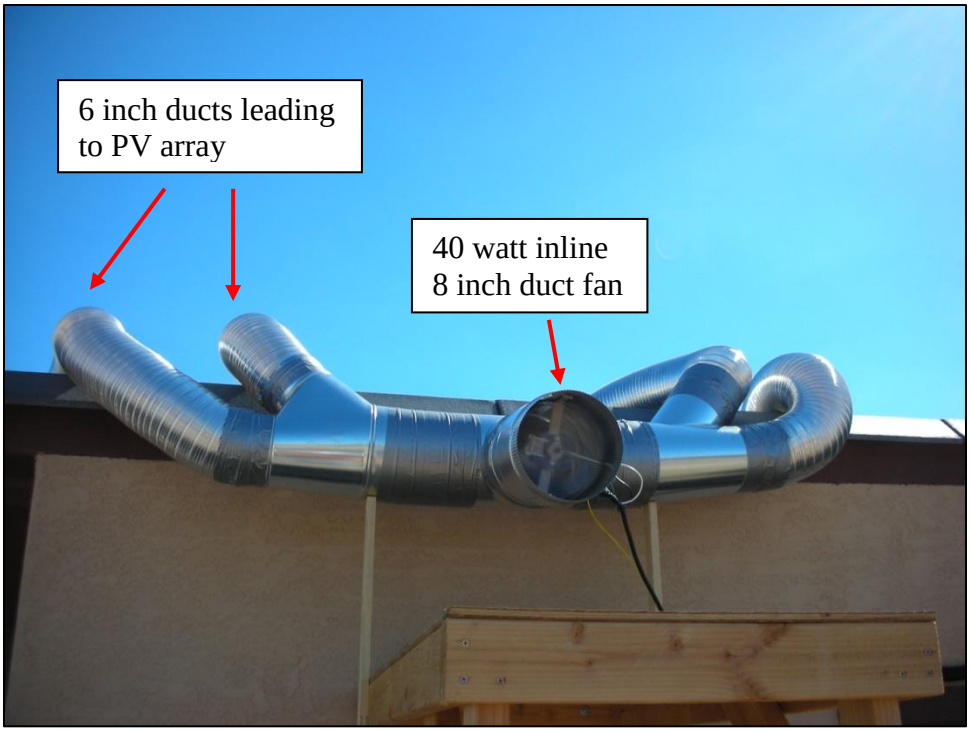

Figure 3.6 Inline Duct Fan and Manifold

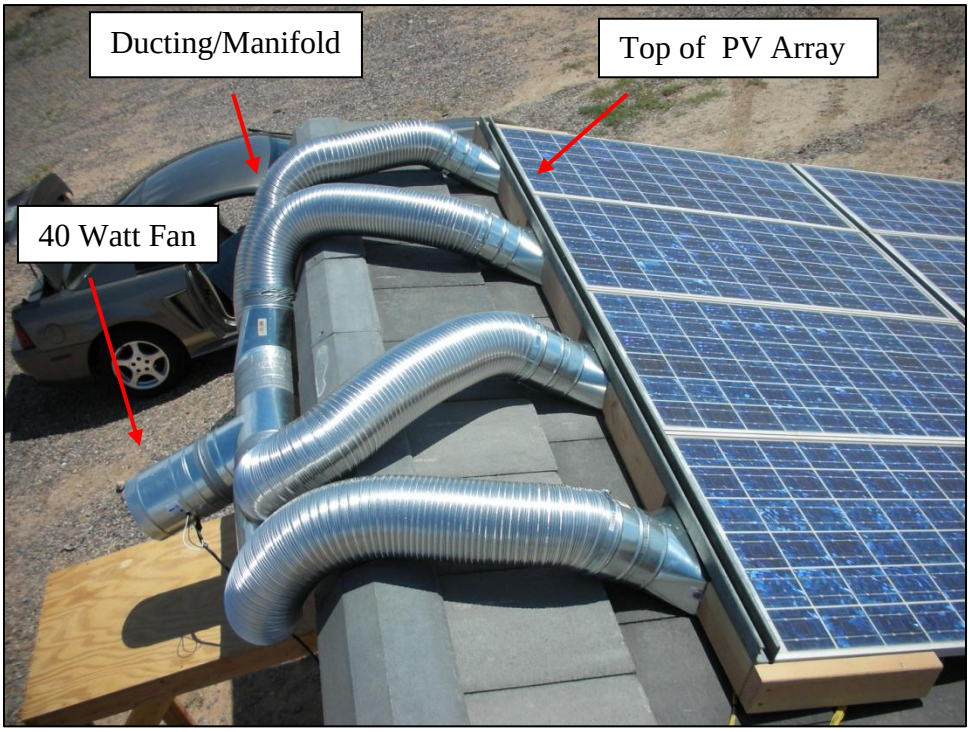

Figure 3.7 Array Ventilation System

Chapter 4

RESULTS & DISCUSSION

4.1 Air Gap Temperature

Residential BAPV systems typically operate at higher temperatures than other types of PV systems due to their close proximity to the rooftop. The incident solar radiation, which is absorbed into the module, is transmitted in the form of heat to the air surrounding the module. Assuming the air behind the module stays relatively stagnant, the temperature of the air gap behind the modules will begin to rise to levels near that of the module (as seen in Figure 4.1). Since the heat energy is confined within the air gap, the overall operating temperature of the modules will remain higher. System designers will typically mount modules at a distance of 1 to 4 inches from the rooftop to allow for ventilation and minimize this effect. Often, the distance in which the modules are mounted is a tradeoff between the aesthetics and performance. Subject to individual preference, modules which are mounted closer to the roof, and have a neater looking appearance, can be more desirable in a residential application. In this project, the modules have been mounted at a distance of 2.5 inches from the roof, which may be a balance between performance and aesthetics. In previous ASU master's thesis, "Temperature of Rooftop PV Modules: Effect of Air Gap and Ambient Condition" by Bijay Lal Shrestha, an air gap of 3 inches is shown to be the optimum distance for which performance gain is achieved for the type of polycrystalline modules used in this project [7].

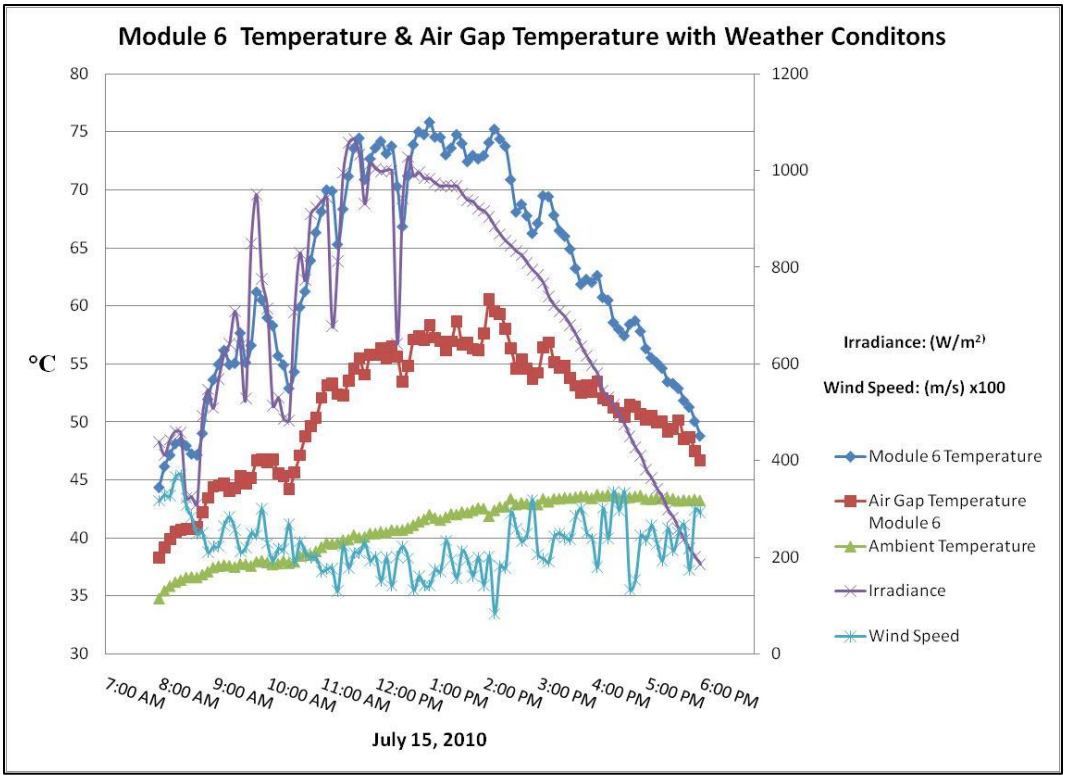

Figure 4.1 Module & Air Gap Temperature July 15, 2010

In Figure 4.1, the air gap temperature of the module is shown to be approximately 15 °C higher than the ambient temperature during the mid-day. The heat exchange rate between the air and the module is being limited by the module's proximity to the roof. If the air gap temperature were equal to the ambient temperature, then the modules would be able to exchange heat with the air at a faster rate. This would allow the modules to operate at a lower temperature. Figure 4.1 also shows the corresponding effects of Irradiance and Wind Speed on the temperature of the module. When the irradiance or wind speed levels increase or decrease, a corresponding module temperature change can be seen.

4.2 Effects of Wind Speed and Direction

The wind speed and direction have an effect on the overall temperature and temperature uniformity of the array as shown in Figure 4.2.

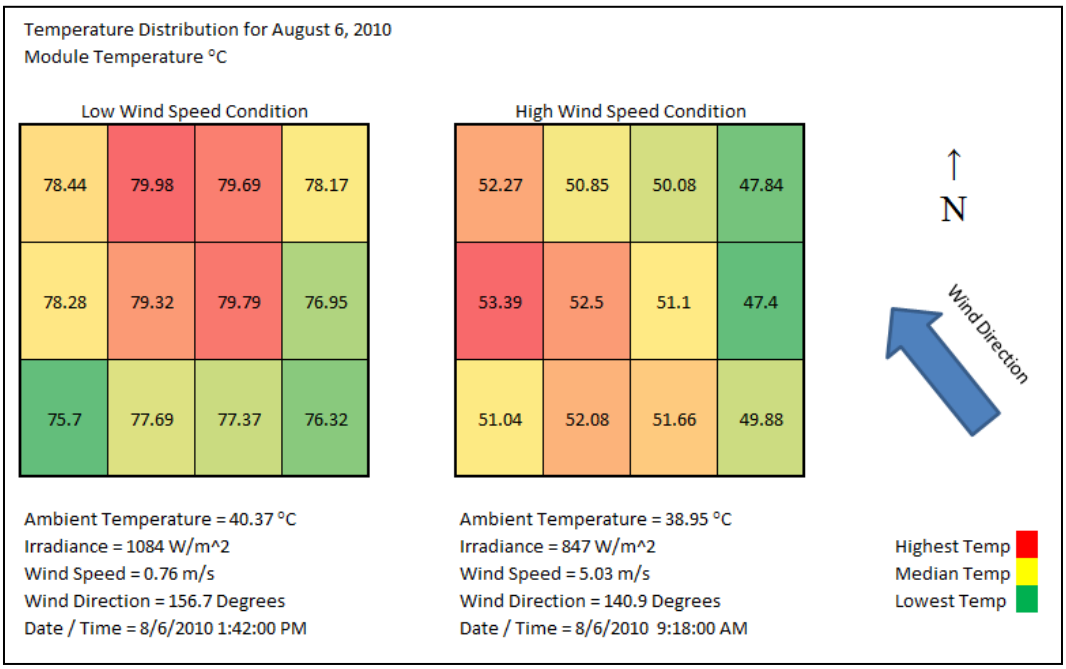

Figure 4.2 Effects of Wind Speed and Direction on Array

In Figure 4.2, the temperature distribution of the array is shown for two different wind speed conditions. During the low speed condition, the temperatures of the modules range from 75.7 to 79.9°C, a difference of 4.2°C, which is slightly more uniform than during the high speed condition where the module temperatures range from 47.4 to 53.4°C, with a difference of 6°C. However, in the low speed condition, it can be seen that the modules on the top row are at a higher temperature than the bottom row. This is due to the 'chimney' effect. Since the roof is pitched at an angle of 23° from horizontal, the heat from the modules will naturally flow up in elevation causing the modules on the top to be warmer. During the high speed condition, it can be seen that the temperature of the

modules is warmest at the end opposite the direction the wind is coming from. It seems that the modules which are hit first by the wind are the coolest and the module with the highest temperature is the point at which the air exits the array.

4.3 Array Thermal Modeling for Temperature Prediction

The thermal model for the array was developed using one month of data from July 15 to August 15. In Arizona, this is the hottest time of the year and it is the time at which the temperature has the greatest effect on the PV modules. The thermal models are based on a linear regression analysis which was done using Predictive Analytics SoftWare (PASW), formerly known as SPSS. The linear regression analysis has three independent variables (Irradiance, Ambient Temperature, and Wind Speed) which are known to effect module temperature. The regression analysis also has a dependent variable which is the Measured Module Temperature. The relation between the dependent and independent variables is what derives the coefficients used in each model. The thermal models can be expressed as shown below in Equation (4.1).

$$T_{module} = E * w_1 + T_{amb} * w_2 + WindSpd * w_3 + c \quad (4.1)$$

Where:

T_{module} = Module Temperature (°C);

E = Irradiance (W/m^2);

T_{amb} = Ambient Temperature (°C);

WindSpd = Wind Speed (m/s);

w_1, w_2, and w_3 = Empirically Derived Coefficients

c = Empirically Derived Constant

A thermal model for each module in the array was developed. Also, an average model was developed using an average of each measured module temperature in the array. The modules were labeled with numbers 1 through 12 as shown in Figure 4.3.

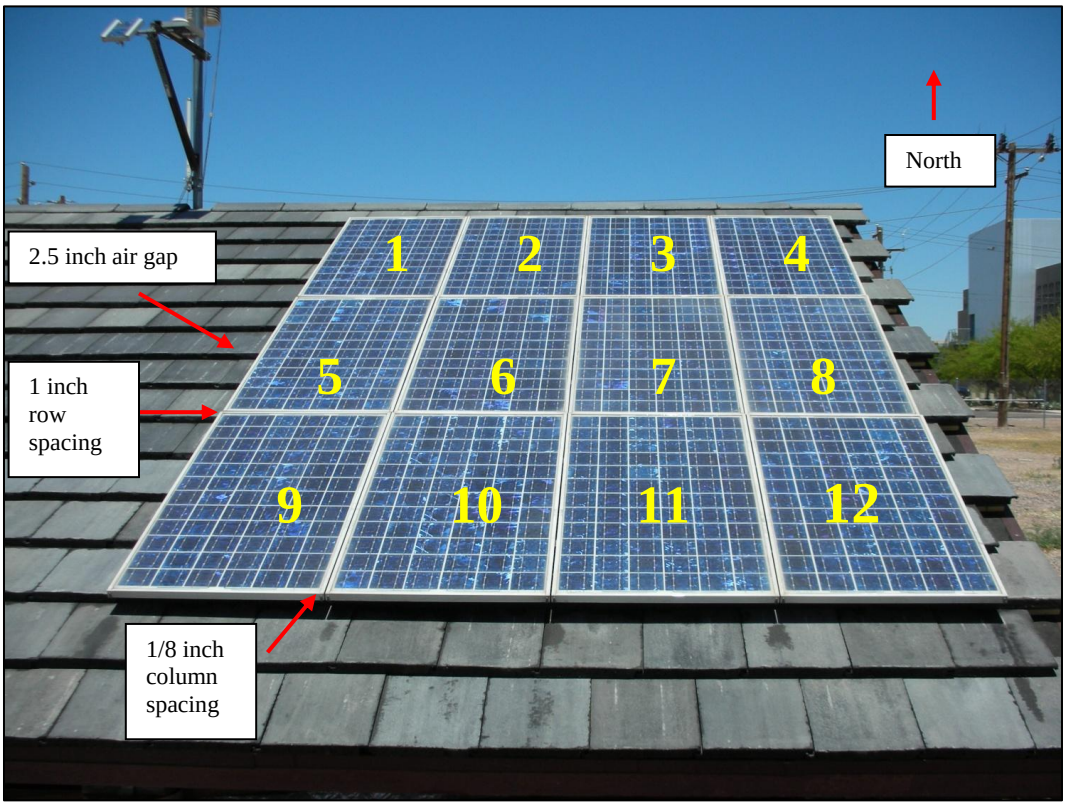

Figure 4.3 Array Layout and Labeling

During the analysis, only data points with Irradiance levels higher than 50 W/m^2 and Wind Speeds lower than 2 m/s were considered. Data points which have Irradiance levels below 50 W/m^2 essentially only occur during the early morning, late evening or night time, and would introduce more variability into the model. The coefficients for each of the independent variables were derived and the results can be seen in Table 4.1.

Table 4.1 Summary of Derived Coefficients (July 15 to Aug 15)

Derived Coefficeints (July 15 to Aug 15)						August 10th, 12:12 pm		
Tmod = E*(w1)+Tamb*(w2)+Windspd*(w3) + C						1027 (W/M2), 37.7°C, 1 m/s		
Module	Irradiance	Tambient	WindSpeed	Constant	R^2 Value	Actual Temp	Predicted Temp	Difference
Module 1	0.031	1.251	-1.603	-5.216	0.948	71.65	71.9	-0.3
Module 2	0.033	1.331	-1.023	-8.462	0.957	75.61	74.8	0.8
Module 3	0.033	1.361	-0.922	-9.348	0.956	75.62	74.6	1.1
Module 4	0.031	1.323	-0.930	-8.184	0.948	72.9	72.7	0.2
Module 5	0.031	1.153	-1.717	-1.825	0.949	70.89	72.1	-1.2
Module 6	0.033	1.226	-1.364	-4.586	0.957	73.75	73.9	-0.2
Module 7	0.034	1.289	-0.960	-7.029	0.959	76.21	75.4	0.8
Module 8	0.031	1.314	-1.051	-7.464	0.956	74.930	73.4	1.6
Module 9	0.028	1.173	-1.696	-2.236	0.948	67.04	68.7	-1.7
Module 10	0.031	1.233	-1.183	-4.941	0.961	72.56	72.6	-0.1
Module 11	0.032	1.275	-1.071	-6.567	0.961	73.4	73.0	0.4
Module 12	0.032	1.264	-1.003	-6.110	0.959	74.44	73.2	1.3
Entire Array	0.032	1.266	-1.210	-5.997	0.960	71.96	73.0	-1.1

After each thermal model equation is developed, an actual data point is plugged into each equation. The result of this spot check of each equation is shown in Table 4.1. All the predicted module temperatures are within ±2°C of the actual module temperatures. In addition to the spot check, a plot of the measured module temperature versus the predicted module temperature is created. The R^2 value of each plot is derived to determine how good the estimated regression equation for each module is. The plot for module number 1 is shown in Figure 4.4 and the plot for the array average temperature is shown in Figure 4.5.

The temperature equation for Module 1 was derived as:

$T_{mod} = E*(0.031) + T_{amb}*(1.251) + WindSpd*(-1.603) – 5.216$

This temperature equation for Module 1 was evaluated in the plot shown in Figure 4.4 and has a R^2 linear value of 0.948.

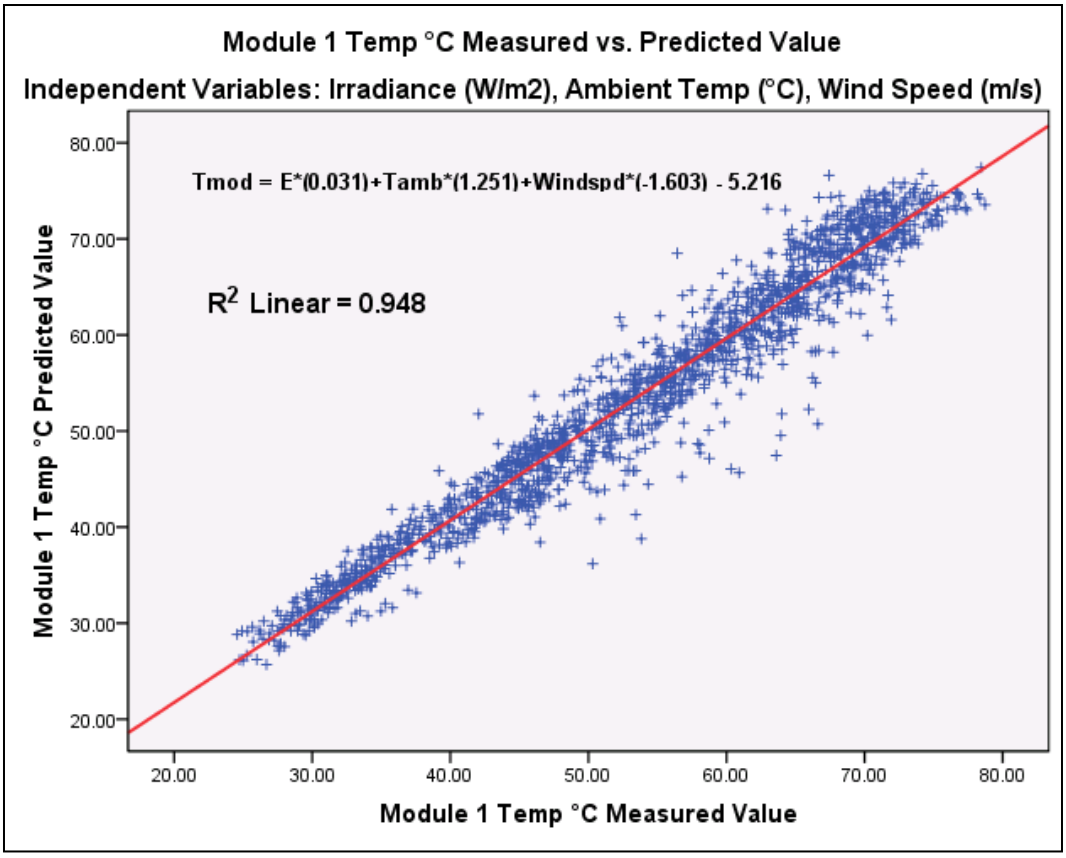

Figure 4.4 Module 1Temperature °C Measured vs. Predicted Value

The temperature equation for the Array Average Temperature was derived as:

T_{array} = E*(0.032) + T_{amb}*(1.266) + Windspd*(-1.210) – 5.997

This temperature equation for the Array Average Temperature was evaluated in the plot shown in Figure 4.5 and has a R^2 linear value of 0.957.

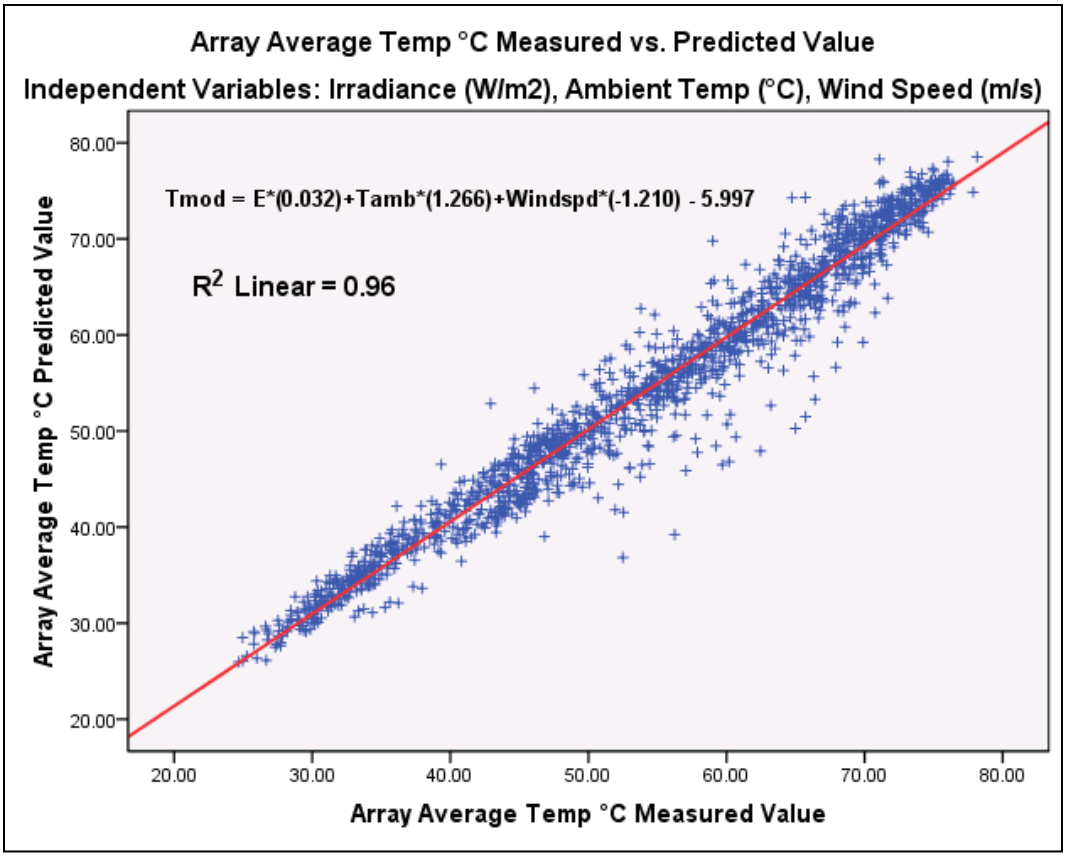

Figure 4.5 Array Average Temperature °C Measured vs. Predicted Value

4.4 Comparison of Coefficients from Two Studies

Another study was done at ASU-PRL by Jaewon Oh [8] which investigates the optimum air gap spacing for sufficiently spaced (2-6inch vertical; 2-inch lateral) modules (2-inch frame depth) of four columns. Each column had modules of the same type and manufacturer, but with air gap (between roof tile and frame bottom) spaces of 0, 1, 2, 3, and 4 inches. Empirically derived coefficients were also derived for this array using the same thermal model equation used in this study. Columns 1 and 3 of Oh's study consisted of polycrystalline silicon modules which are comparable to the modules used for the

2.5 inch air gap array used in this study. A comparison of the coefficients derived from both studies is shown in Table 4.2.

Table 4.2 Comparison of Coefficients between Two Studies

Coefficient Comparison Between Two Studies (Hrica and Oh)					1027 (W/M2), 37.7°C, 1 m/s	
	Irradiance	Tambient	WindSpeed	Constant	Actual Module Temp	Predicted Module Temp
Column A 2.5" Air Gap* (Module 5)	0.031	1.153	-1.717	-1.825	70.89	72.12
Column A 2" Air Gap**	0.029	1.308	-1.342	-9.129	n/a	68.11
Column A 3" Air Gap**	0.030	1.228	-1.629	-6.963	n/a	68.39
	Irradiance	Tambient	WindSpeed	Constant		
Column C 2.5" Air Gap* (Module 7)	0.034	1.289	-0.960	-7.029	76.21	75.44
Column C 2" Air Gap**	0.034	1.363	-0.912	-6.426	n/a	79.16
Column C 3" Air Gap**	0.030	1.551	-1.941	-9.982	n/a	77.17
*Data range = July 15 to Aug 15						
**Data from study at ASU-PRL by Jaewon Oh [8], Data range = Aug 1 to Aug 15						
All Coefficients Derived for Data Points with Wind Speed below 2 m/s and Irradiance above 50 W/m^2						

The comparison of coefficients in Table 4.2 shows that the thermal models generated in each study predicts module temperatures within 4°C of each other for typical weather conditions during August in Arizona. A slight difference is expected due to a difference in measurement of module temperature between the two studies: Oh's study measured the cell temperature of the module directly, whereas this study measured the backsheet temperature of the module.

A quick experiment was conducted to compare measured cell temperature versus backsheet temperature for the polycrystalline silicon modules used in this experiment. One thermal couple was placed directly on the cell by cutting a small hole in the backsheet, while another thermal couple was adhered to the backsheet of an adjacent cell. This module was then placed on an open rack two-axis tracker for a period of 15 minutes and allowed to reach thermal equilibrium under the given irradiance and weather conditions. Ten temperature measurements from each thermal couple were measured using a single multi-meter. The results of this experiment are shown in Table 4.3.

Table 4.3 Measured Backsheet Temperature vs. Cell Temperature

Cell Temp °C	Back Sheet Temp °C	Difference
49.9	48.5	1.4
50.5	48.7	1.8
51.3	48.7	2.6
51.5	50.6	0.9
52.3	50.9	1.4
52.5	51.3	1.2
52.6	51.2	1.4
52.7	51.4	1.3
52.8	51.3	1.5
52.9	51.2	1.7
	Average Difference:	1.52

The data in Table 4.3 shows that the measured cell temperature is approximately 1.5°C higher than measured backsheet temperature. This temperature difference can account for some of the variance in the thermal models between studies.

Additional variances can be attributed to the difference in the vertical and lateral spacing between modules between the two studies. The modules in Jaewon Oh's study had 2 to 6-inch vertical and 2-inch lateral spacing, and the modules in this experiment had 1-inch vertical and 1/8-inch lateral spacing. Modules which have closer vertical and lateral spacing are expected to operate at higher temperatures due to their close proximity and minimal ventilation. Even further variance can be expected due to the difference in manufacture (materials used, color, density, etc.) between the modules used in each study.

Despite the possible causes of variance between the two studies, there is only a 4°C difference in predicted temperature. A longer term study which involves the comparison of two arrays with identical modules and identical measurement methods used may reveal even greater accuracy.

4.5 Fan Effect

4.5.1 Fan Effect Phase 1 Experiments – Thermal Modeling

The evaluation of the fan effect on the array was divided into two phases. In phase 1, the ducting and fan structure was attached to the top of the array and the fan was left in the OFF position for a period of 7 days, as baseline temperature data was collected. Then the fan was in the ON position for a period of 7 days while additional temperature data was collected. Thermal models for the array were created for each of the two 7 day periods using the same process described in section 4.3 of this document.

The temperature equation for predicting the Array Average Temperature while the fan was in the OFF and ON positions were derived and are shown in Table 4.2

Table 4.4 Thermal Models for Fan in OFF and ON Positions

Fan Position	Thermal Equation	R^2 Value
OFF	Tarray = E*(0.029)+Tamb*(1.530)+WindSpd*(-2.717)-9.095	0.953
ON	Tarray = E*(0.030)+Tamb*(1.450)+ WindSpd*(-3.608)-9.759	0.925

The expected difference in these equations is that the equation for when the fan is ON will predict a cooler temperature for the array than the equation for when the fan is OFF. This result turns out to be the case as shown in Table 4.3, by plugging the same Irradiance, Ambient Temperature, and Wind Speed values into each equation, the predicted value of the average array temperature is on the order of 3 to 4°C cooler when the fan is in the ON position when compared to the OFF position.

Table 4.5 Predicted Array Average Temperature Using Derived Equations

Inputs			Predicted Temperature °C		Temperature Change °C
Irradance (W/m^2)	Tamb °C	WindSpd (m/s)	Fan OFF	Fan On	(Fan OFF) - (Fan On)
1000	40	1	78.39	74.63	3.76
900	35	1	67.84	64.38	3.46
800	32	1	60.35	57.03	3.32
700	30	1	54.39	51.13	3.26

A temperature decrease of 3 to 4°C on the array may seem small, but when considering the effect it could have on the efficiency the improvement in total power output and lifetime of an array could be great. Since photovoltaic modules typically lose 0.5% efficiency per °C, a temperature drop of 3.5°C corresponds to a 1.75% increase in efficiency. Table 4.4 shows the corresponding increase in power output for arrays at various sizes due to an efficiency increase of 1.75%

Table 4.6 Effect of Efficiency Gain (%) on Power Output

Array Size (kW)	Application	Efficiency Gain (%)	Power Output Gain (W)
5 kW	Residential	1.75	87.5
50 kW	Commercial	1.75	875
200 kW	Industrial	1.75	3500

The rated power output of the array used in this experiment was 1.2 kW and a 1.75% improvement in efficiency correlates to a 21 Watt improvement in power output for this particular array. This does not make up for the 40 Watts which were used to power the fan. However, the modules used in this experiment have a relatively low efficiency rating of 10.5% at standard operating conditions. This means that they take up a lot of space with low power output. Newer modules with higher efficiencies may be able to produce nearly double the power output using the same space. For example if the rated output of the test array were actually 2.4 kW, then the 1.75% improvement in efficiency would correlate to a 42 Watt improvement in power. This improvement would then at least break even

with the fans power consumption. Fine tuning of a system of this type, or using a pulse control on the fan could possibly lead to a net gain in power. All these power gain calculations have been done for 2.5-inch air gap; however, the power gain is expected to be much higher for the 1-inch air gap arrays which are preferred by many system integrators because of low wind loading and better aesthetic reasons.

4.5.2 Fan Effect on Array Temperature Uniformity

As discussed in Section 4.2, the array has a non-uniform temperature distribution at low wind speed conditions in which the modules in the top row of the array have a higher temperature than the bottom row. The fan has an effect of reducing this non-uniformity of the array as shown in Figure 4.6.

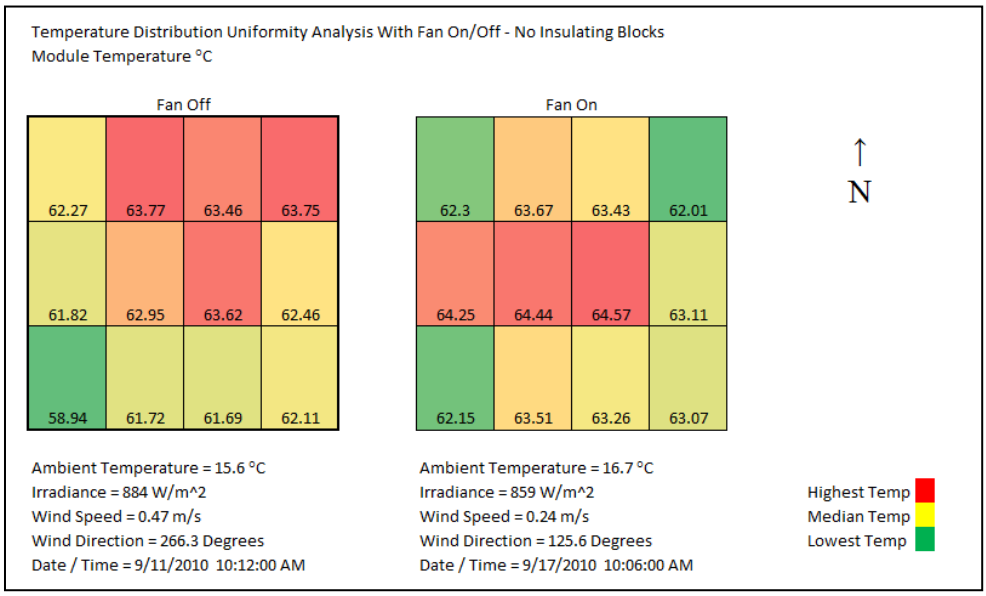

Figure 4.6 Fan Effect on Array Temperature Uniformity

In Figure 4.6, similar ambient conditions and times of day were selected for the comparison of the OFF and ON positions. It can be seen the fan is reducing the non-uniformity by providing more ventilation to the array. When the fan is on, the

module temperatures range from 58.9 to 63.8°C, a difference of 4.9°C. When the fan is on, the module temperatures range from 64.6 to 62.0°C, a difference of 2.6°C. However, by looking at this temperature distribution, only the top row of the array seems to be effected by the fan. This is likely due to air entering from the sides of the top row of the array. Later in the experiment, insulating blocks were added to the side of the array as shown in Figure 4.7 so that the air would enter the array from the bottom, rather than the sides.

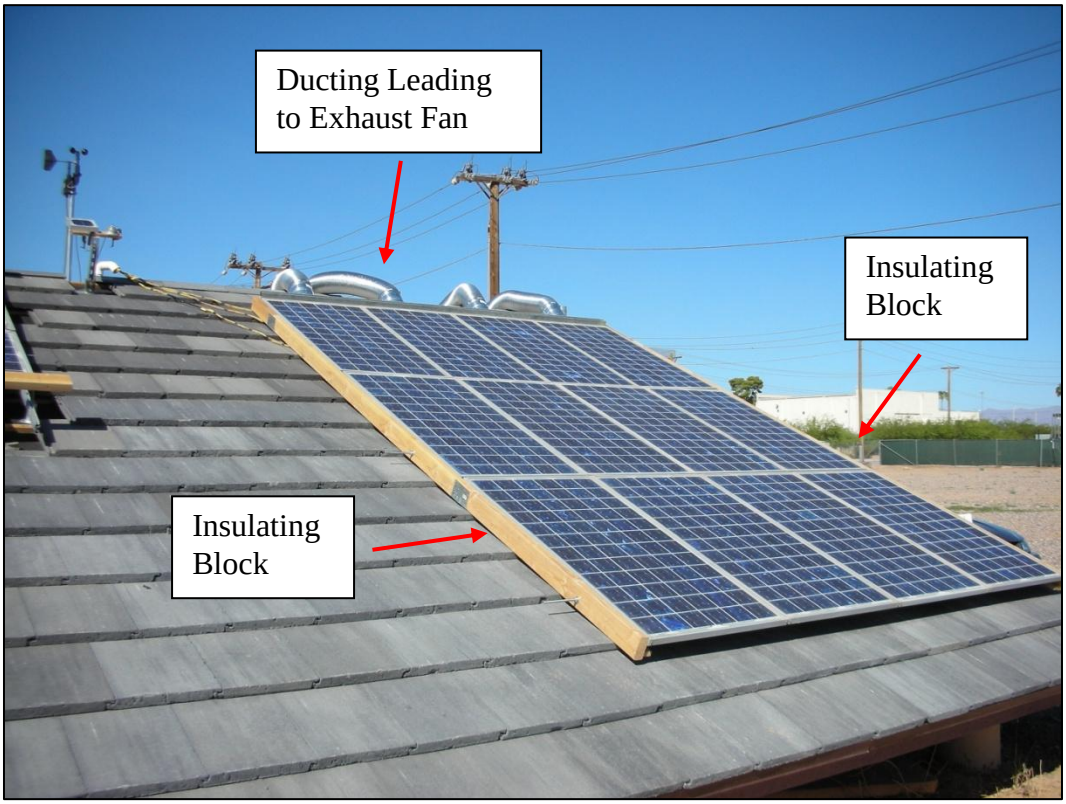

Figure 4.7 Array with Insulating Blocks on Sides

The result of adding the blocks to the sides of the array is shown in Figure 4.8.

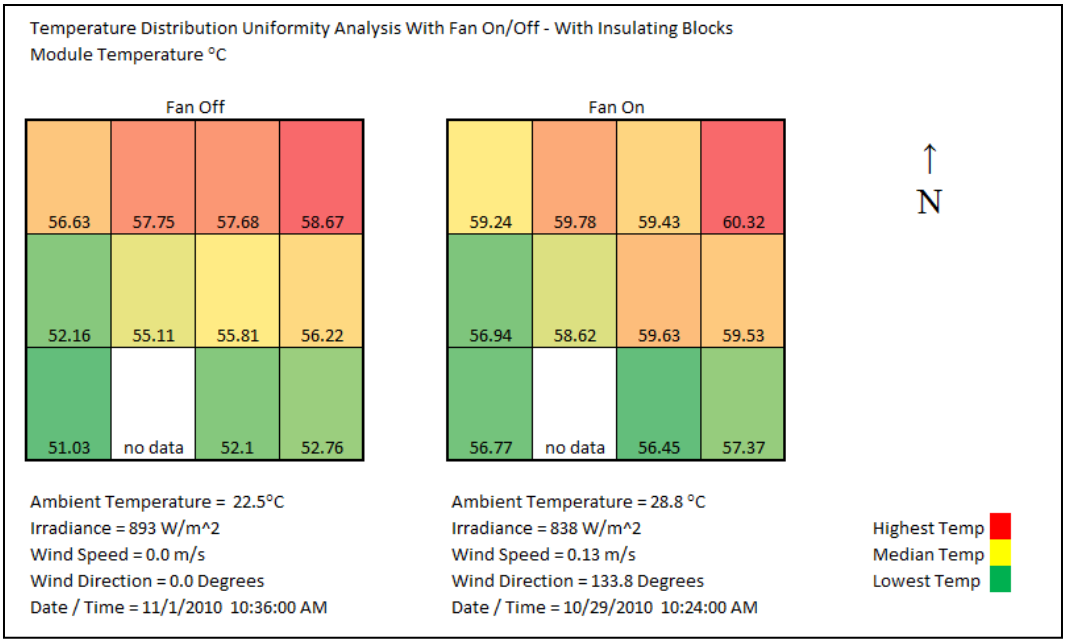

Figure 4.8 Fan Effect on Temperature Uniformity with Insulating Blocks

In Figure 4.8, similar ambient conditions were chosen to compare the array uniformity with the fan in the OFF and ON positions. This comparison was done with insulating blocks on the side of the array. When the fan is off, the module temperature range is from 51.0 to 58.7°C, a difference of 7.7°C. When the fan is on, the module temperature range is from 56.8 to 60.3°C, a difference of 3.5°C. This figure shows that there is a more uniform temperature distribution with the fan on and with the insulating blocks in place.

When comparing Figures 4.6 and 4.8 with the fan in the on position, it is likely that the air is entering from the bottom of the array and moving to the top with the blocks in place, rather than entering from the sides. This allows for an even more uniform temperature distribution.

4.5.3 Fan Effect Phase 2 Experiments – Efficiency Measurements

In phase 2, several experiments were conducted in which the fan was turned ON and OFF in 15 minute intervals. In this phase of the experiment, insulating blocks were added to the side of the array to reduce the effect of the wind conditions so that the effect of the fan could be more clearly measured. The peak power output of each of the three sub-arrays (Top, Middle, and Bottom) and the entire array was measured using a Daystar Photovoltaic Curve Tracer. The peak power output was matched with the Irradiance data to determine the array efficiency. The expected outcome of the experiments was that when the fan was in the ON position the efficiency of each array would increase. This result can be seen in the plots in Figures 4.9 through 4.12.

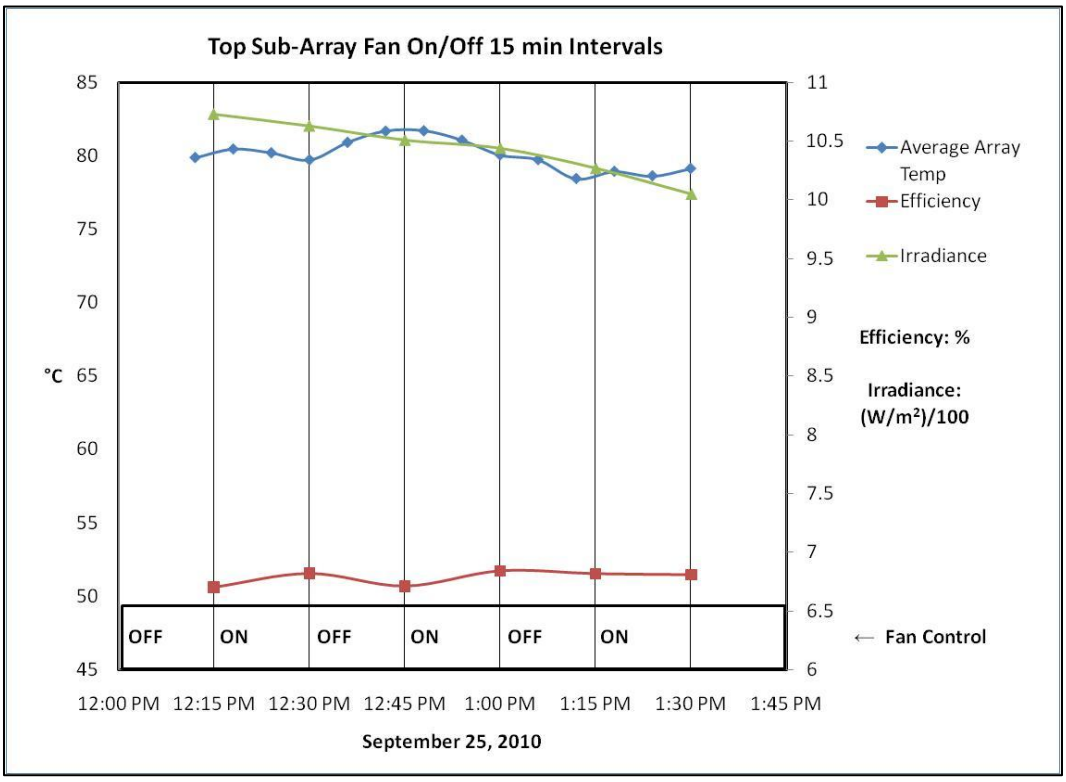

Figure 4.9 Top-Sub Array Efficiency with 15 min Fan ON/OFF

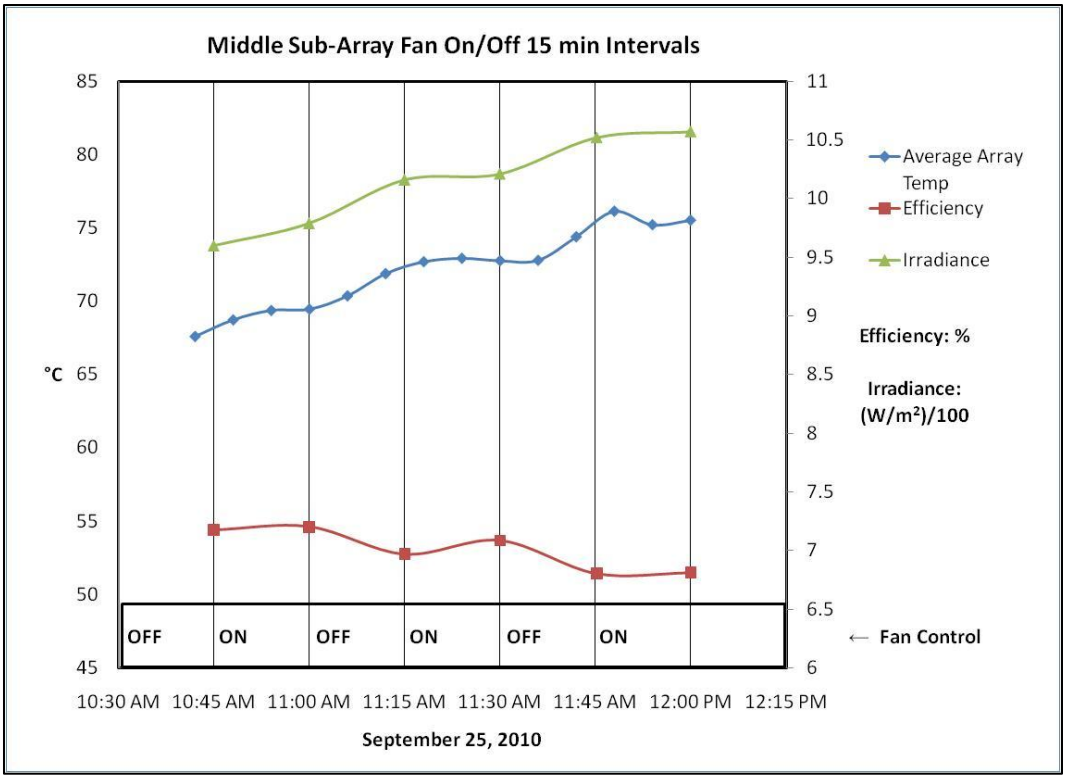

Figure 4.10 Middle-Sub Array Efficiency with 15 min Fan ON/OFF

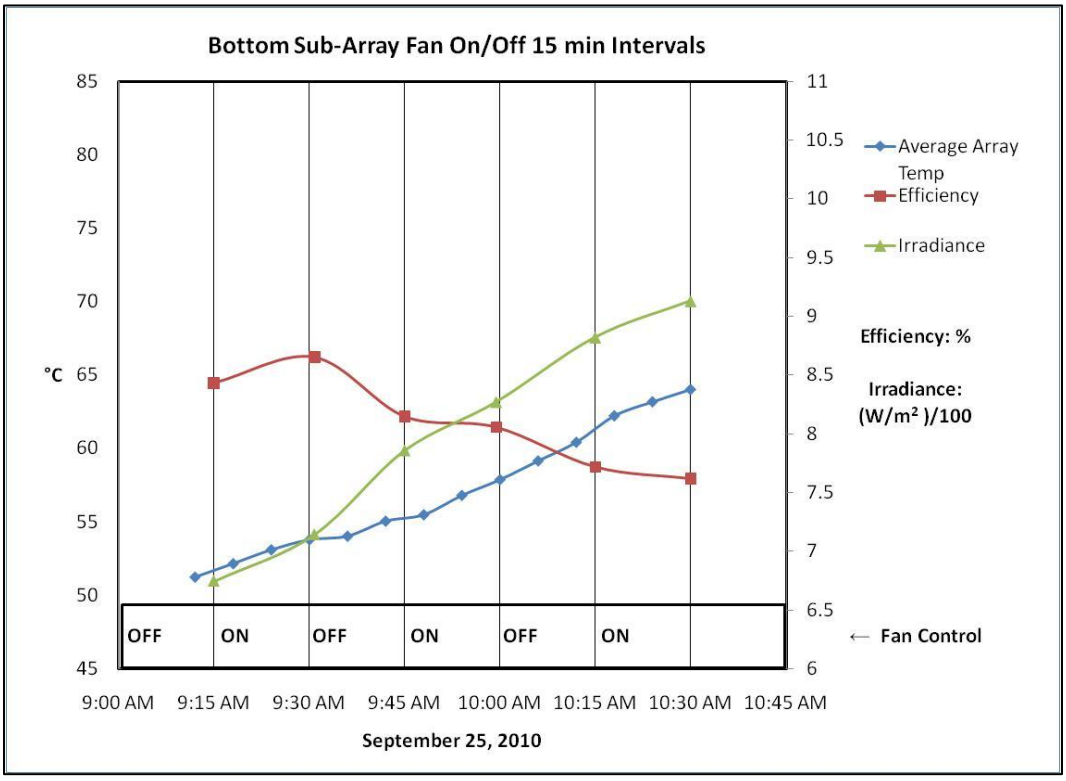

Figure 4.11 Bottom-Sub Array Efficiency with 15 min Fan ON/OFF

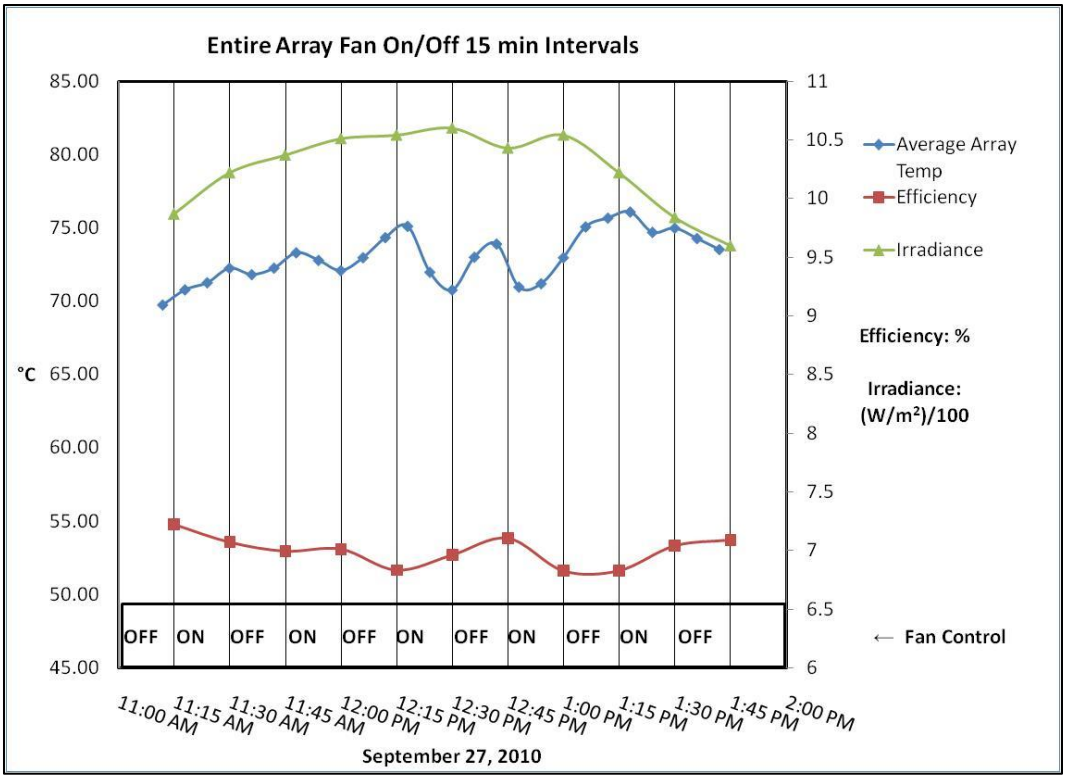

Figure 4.12 Entire Array Efficiency with 15 min Intervals Fan ON/OFF

In general, there is a slight increase in efficiency when the fan is in the ON position vs. when the fan is OFF. However, in some instances the change in ambient conditions may be having a greater effect on efficiency than the fan. Each efficiency plot has been normalized for irradiance, since the measured irradiance is included in the efficiency calculation. However, the effect of changing wind speed and ambient temperature may be aiding or hindering the results shown in each interval. In any case, the efficiency gains are only on the order of 0.5 to 1% which is not a sufficient improvement to make up for the power being consumed by the fan itself. A 1.2 kW array such as this would need to see at least a 3.3% improvement in efficiency in order to break even with the 40-Watts of power being consumed by the fan.

The length of the fan intervals was also considered. It is possible that the short 15 minute intervals were not long enough to give the fan sufficient time to cool the thermal mass of the modules. In order to determine if longer fan intervals would increase the fan effect, another experiment was done with 45 minute intervals. However, the results of this experiment did not show any additional improvement in efficiency over the 15 minute intervals.

Chapter 5

CONCLUSIONS & RECOMENDATIONS

5.1 Conclusions

The high operating temperature of BAPV modules has a direct impact on the performance and long term reliability of a BAPV system. A thermal model has been developed in this study, which can be useful in predicting the operating temperature of similar arrays under a given set of ambient conditions. This temperature prediction can be used for providing more accurate estimates of the lifetime performance and reliability of BAPV systems. In addition, the effect of cooling an array with an exhaust fan has been evaluated. Although, the fan did not have much effect on power or efficiency, there was a significant effect on the temperature uniformity of the array. This improvement in temperature uniformity could lead to improvements in array performance as the mismatch factor is reduced. The fan also had an effect of lowering the average temperature of the array. Further study could reveal great improvements in array lifetime reliability with lower lifetime operating temperatures.

5.2 Recommendations

Further investigation is needed to determine the potential effects of a cooling fan on array temperature uniformity and the lifetime reliability of BAPV modules. A long term study should be carried out with two identical BAPV arrays with 1-inch air gap. One array should have a fan cooling system, the other without. A side by side comparison may reveal the potential benefits associated with increased temperature uniformity and lower average operating temperatures.

REFERENCES

[1] Honsberg, Christiana, and Stuart Bowden. *PV CDROM - Solar Cell Operation: Effect of Temperature.* 2010. http://www.pveducation.org/pvcdrom/solar-cell-operation/effect-of-temperature (accessed 10 30, 2010).

[2] Mehalic, Brian. "Seeking Peak Performance: Lowing the Cost of Grid-Tied PV Systems." *Home Power*, October/November 2009: 50-55.

[3] Messenger, Roger A., and Jerry Ventre. "Photovoltaic Systems Engineering: Second Edition." 54. New York: CRC Press, 2003.

[4] King, D.L., W.E. Boyson, and J.A. Kratochvil. *PHOTOVOLTAIC ARRAY PERFORMANCE MODEL.* Albuquerque, New Mexico: Sandia National Laboratories, 2004.

[5] TamizhMani, Govindasamy, Liang Ji, Yingtang Tang, Luis Petacci, and Carl Osterwald. "PHOTOVOLTAIC MODULE THERMAL/WIND PERFORMANCE: Long -Term Monitoring and Model Development For Energy Rating." *NCPV and Solar Program Review Meeting.* Denver, CO, 2003. 936-939.

[6] Tang, Yingtang. *Outdoor Energy Rating Measurements of Photovoltaic Modules.* Master's Thesis, Tempe, AZ: Arizona State University, 2005.

[7] Shrestha, Bijay. *Temperature of Rooftop PV Modules: Effect of Air Gap and Ambient Condition* . Master's Thesis, Tempe, AZ: Arizona State University, 2009.

[8] Oh, Jaewon. *Building Applied and Back Insulated Photovoltaic Modules: Thermal Models* . Master's Thesis, Tempe, AZ: Arizona State University, 2010.

APPENDIX A

LINEAR REGRESION PLOTS

This appendix contains the linear regression analysis plots for the derived coefficients for modules 1 though 12 and the entire array.

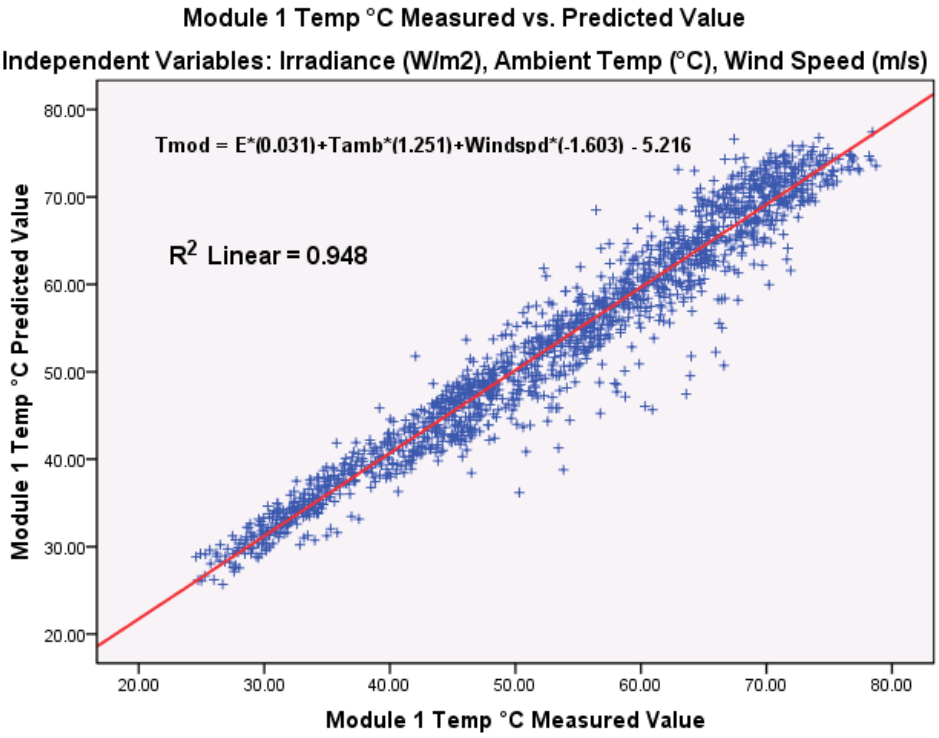

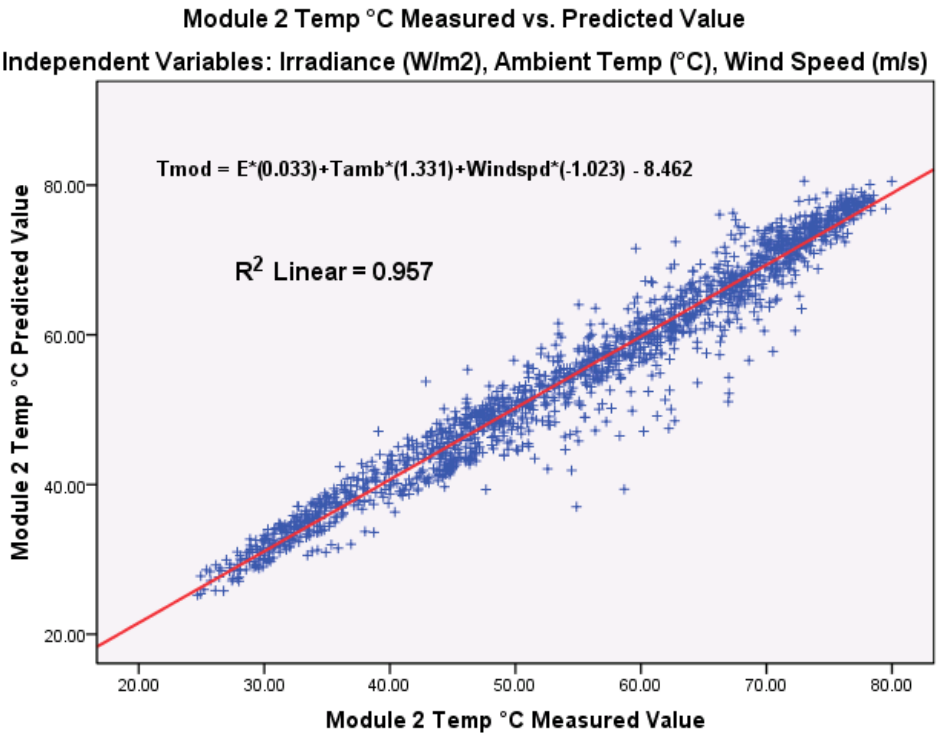
Module 2 Temp °C Measured vs. Predicted Value
Independent Variables: Irradiance (W/m2), Ambient Temp (°C), Wind Speed (m/s)
Tmod = E*(0.033)+Tamb*(1.331)+Windspd*(-1.023) - 8.462
R2 Linear = 0.957
Module 2 Temp °C Predicted Value
Module 2 Temp °C Measured Value
20.00
30.00
40.00
50.00
60.00
70.00
80.00

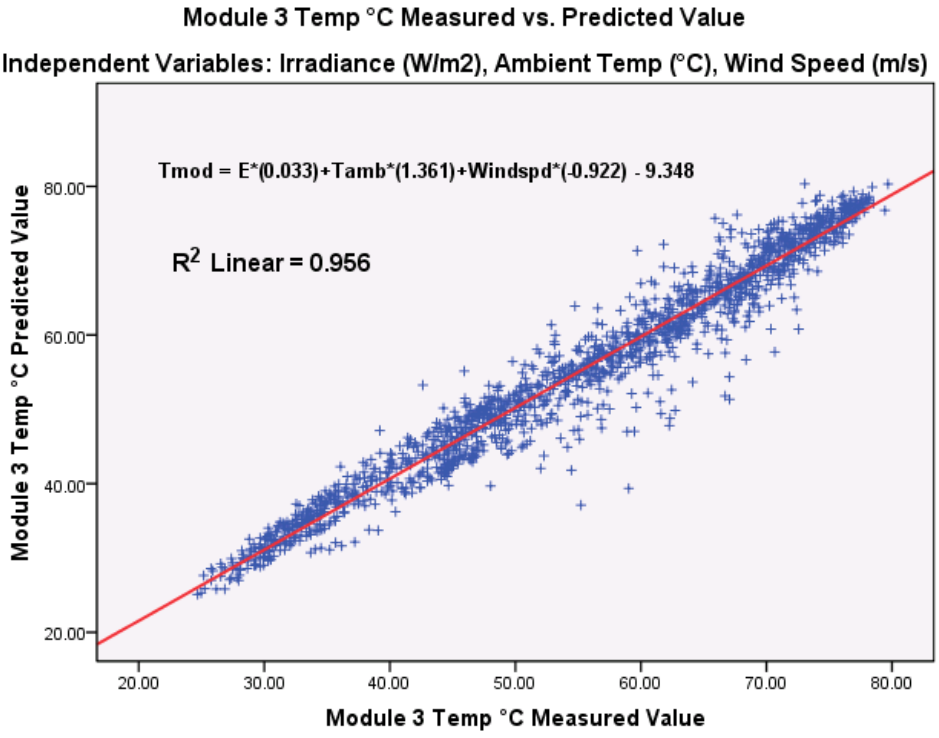
Module 3 Temp °C Measured vs. Predicted Value
Independent Variables: Irradiance (W/m2), Ambient Temp (°C), Wind Speed (m/s)
Tmod = E*(0.033)+Tamb*(1.361)+Windspd*(-0.922) - 9.348
R2 Linear = 0.956
Module 3 Temp °C Predicted Value
Module 3 Temp °C Measured Value
20.00
30.00
40.00
50.00
60.00
70.00
80.00

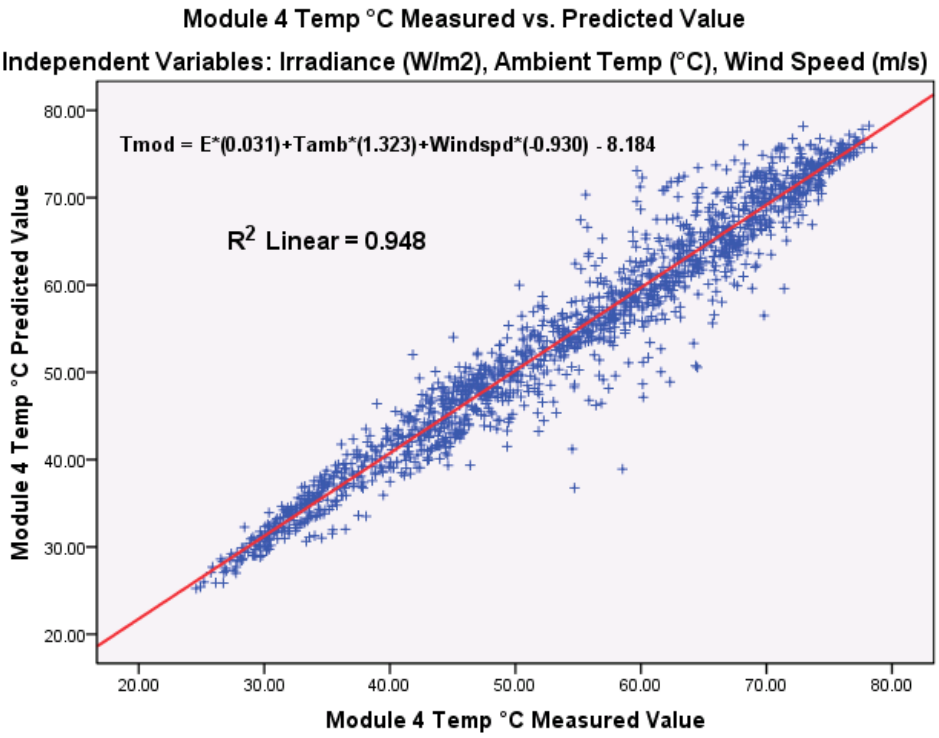
Module 4 Temp °C Measured vs. Predicted Value
Independent Variables: Irradiance (W/m2), Ambient Temp (°C), Wind Speed (m/s)
Tmod = E*(0.031)+Tamb*(1.323)+Windspd*(-0.930) - 8.184
R2 Linear = 0.948
Module 4 Temp °C Predicted Value
Module 4 Temp °C Measured Value
80.00
70.00
60.00
50.00
40.00
30.00
20.00
20.00
30.00
40.00
50.00
60.00
70.00
80.00

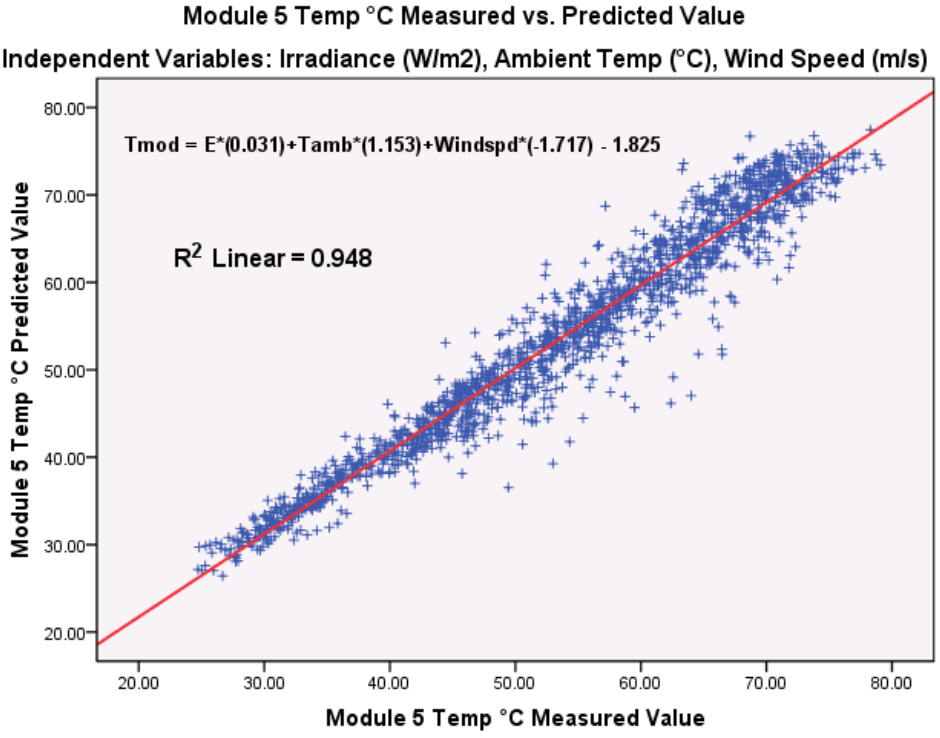
Module 5 Temp °C Measured vs. Predicted Value
Independent Variables: Irradiance (W/m2), Ambient Temp (°C), Wind Speed (m/s)
Tmod = E*(0.031)+Tamb*(1.153)+Windspd*(-1.717) - 1.825
R2 Linear = 0.948
Module 5 Temp °C Predicted Value
Module 5 Temp °C Measured Value
80.00
70.00
60.00
50.00
40.00
30.00
20.00
20.00
30.00
40.00
50.00
60.00
70.00
80.00

Module 6 Temp °C Measured vs. Predicted Value

Independent Variables: Irradiance (W/m2), Ambient Temp (°C), Wind Speed (m/s)

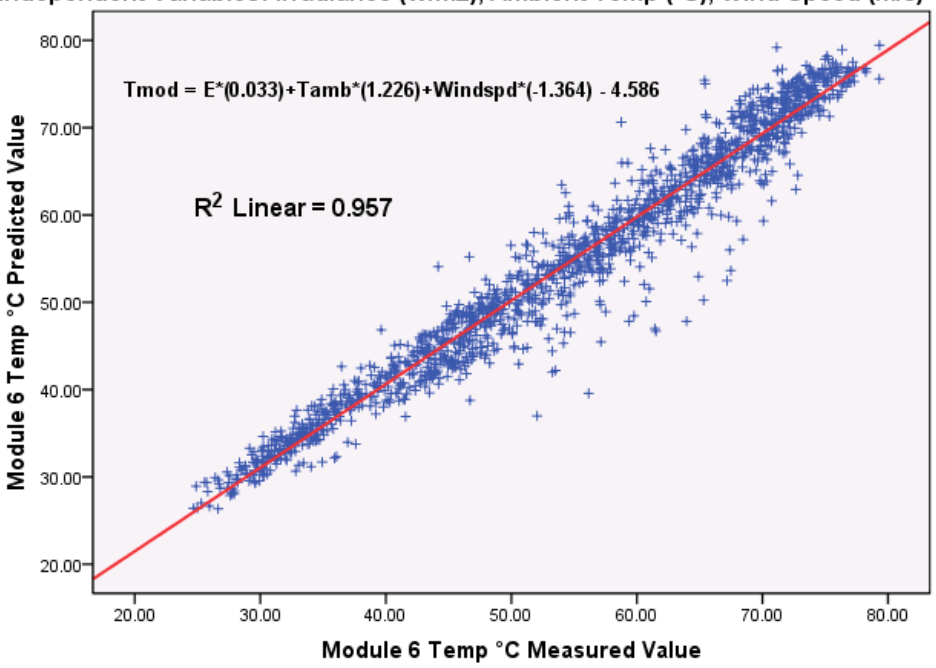

Module 7 Temp °C Measured vs. Predicted Value

Independent Variables: Irradiance (W/m2), Ambient Temp (°C), Wind Speed (m/s)

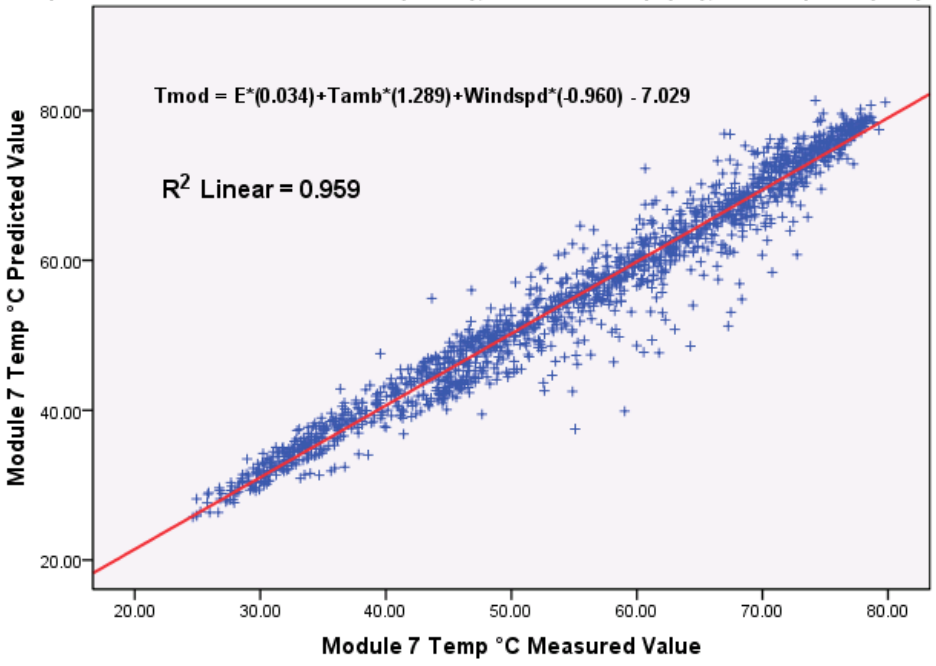

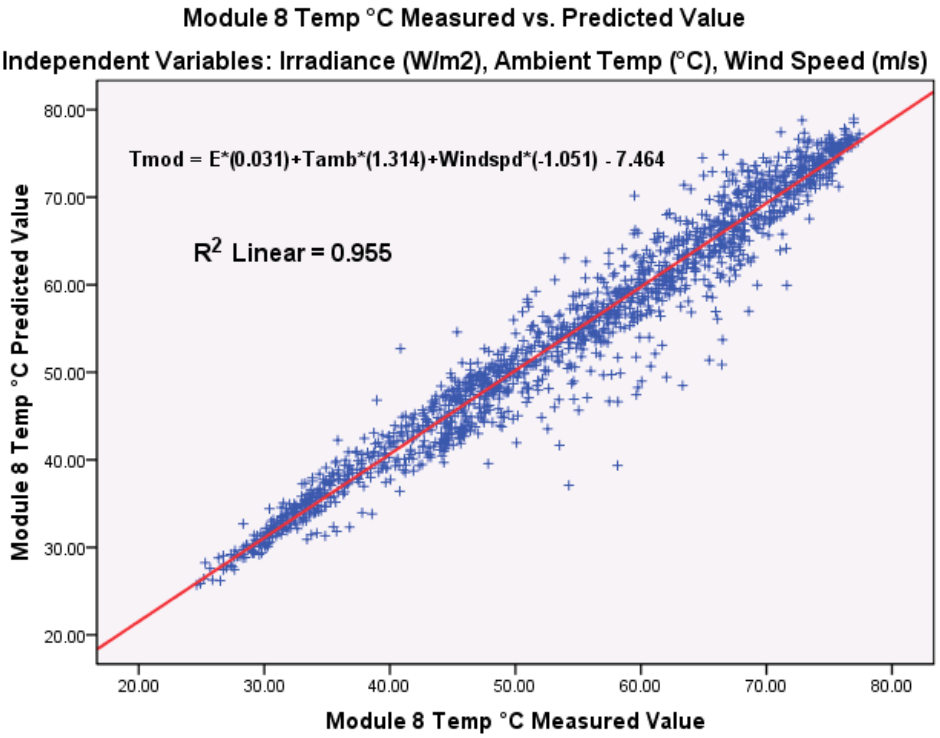
Module 8 Temp °C Measured vs. Predicted Value
Independent Variables: Irradiance (W/m2), Ambient Temp (°C), Wind Speed (m/s)
Tmod = E*(0.031)+Tamb*(1.314)+Windspd*(-1.051) - 7.464
R2 Linear = 0.955
Module 8 Temp °C Predicted Value
Module 8 Temp °C Measured Value
80.00
70.00
60.00
50.00
40.00
30.00
20.00
20.00
30.00
40.00
50.00
60.00
70.00
80.00

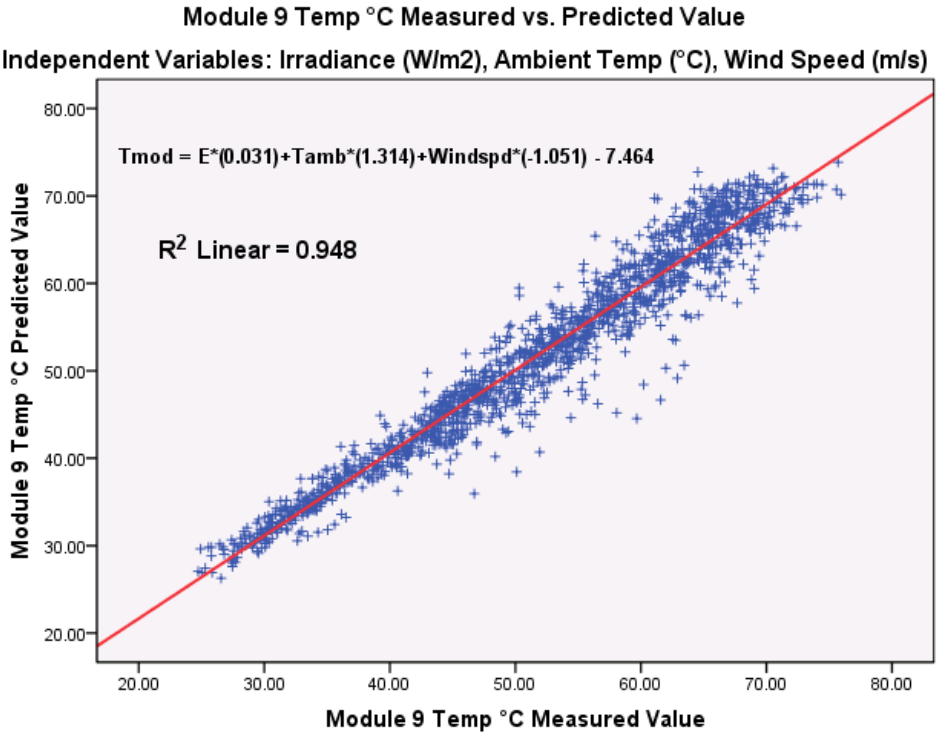
Module 9 Temp °C Measured vs. Predicted Value
Independent Variables: Irradiance (W/m2), Ambient Temp (°C), Wind Speed (m/s)
Tmod = E*(0.031)+Tamb*(1.314)+Windspd*(-1.051) - 7.464
R2 Linear = 0.948
Module 9 Temp °C Predicted Value
Module 9 Temp °C Measured Value
80.00
70.00
60.00
50.00
40.00
30.00
20.00
20.00
30.00
40.00
50.00
60.00
70.00
80.00

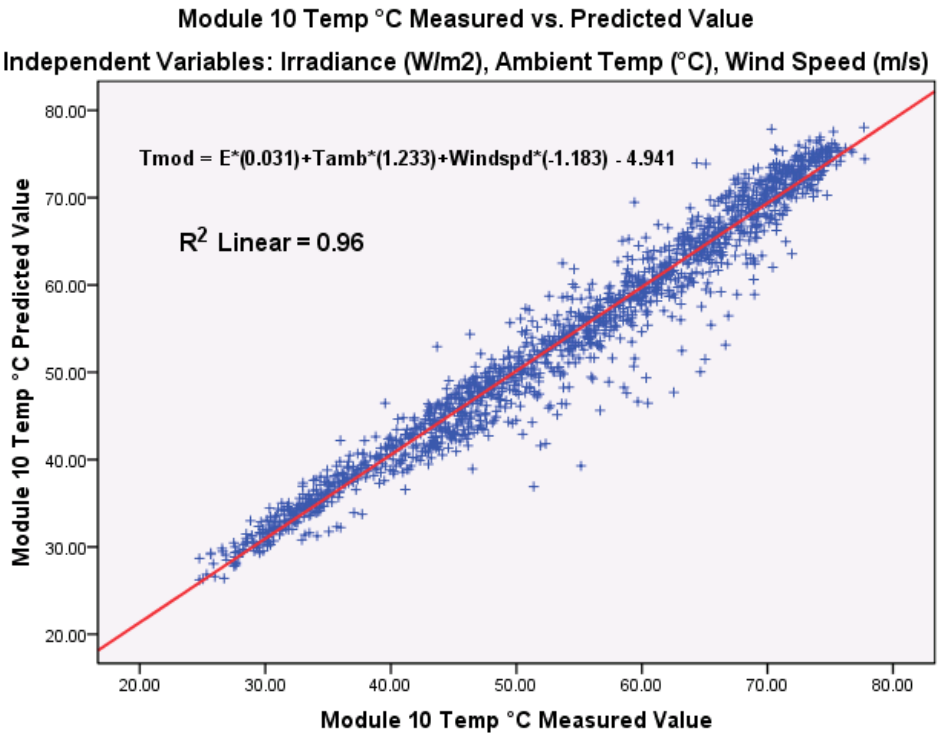
Module 10 Temp °C Measured vs. Predicted Value
Independent Variables: Irradiance (W/m2), Ambient Temp (°C), Wind Speed (m/s)
Tmod = E*(0.031)+Tamb*(1.233)+Windspd*(-1.183) - 4.941
R2 Linear = 0.96
Module 10 Temp °C Predicted Value
Module 10 Temp °C Measured Value
20.00
30.00
40.00
50.00
60.00
70.00
80.00

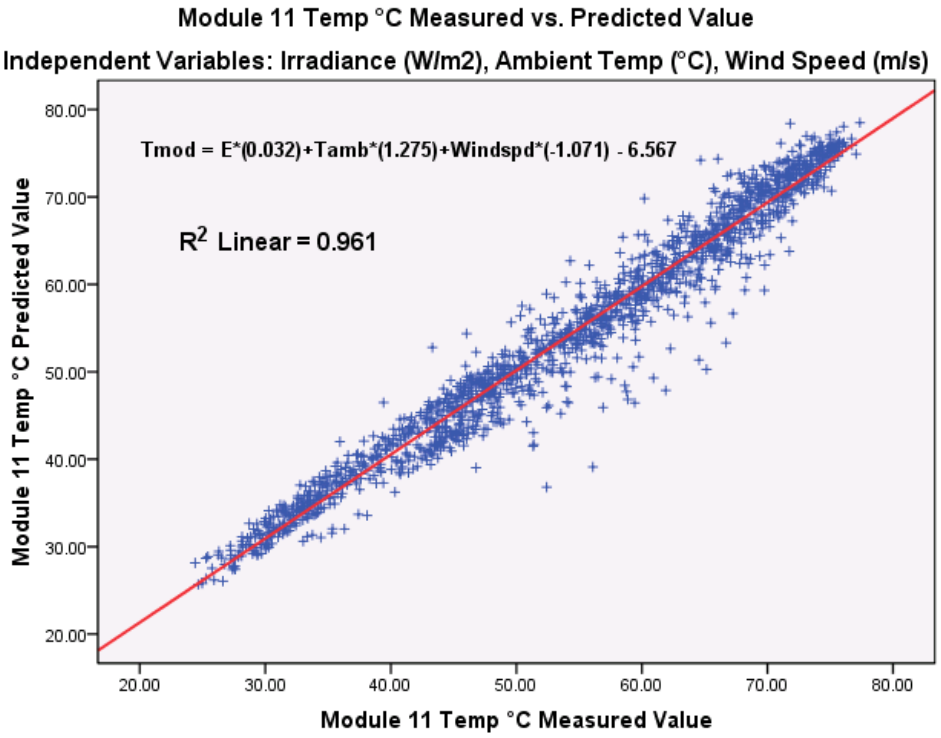
Module 11 Temp °C Measured vs. Predicted Value
Independent Variables: Irradiance (W/m2), Ambient Temp (°C), Wind Speed (m/s)
Tmod = E*(0.032)+Tamb*(1.275)+Windspd*(-1.071) - 6.567
R2 Linear = 0.961
Module 11 Temp °C Predicted Value
Module 11 Temp °C Measured Value
20.00
30.00
40.00
50.00
60.00
70.00
80.00

Module 12 Temp °C Measured vs. Predicted Value

Independent Variables: Irradiance (W/m2), Ambient Temp (°C), Wind Speed (m/s)

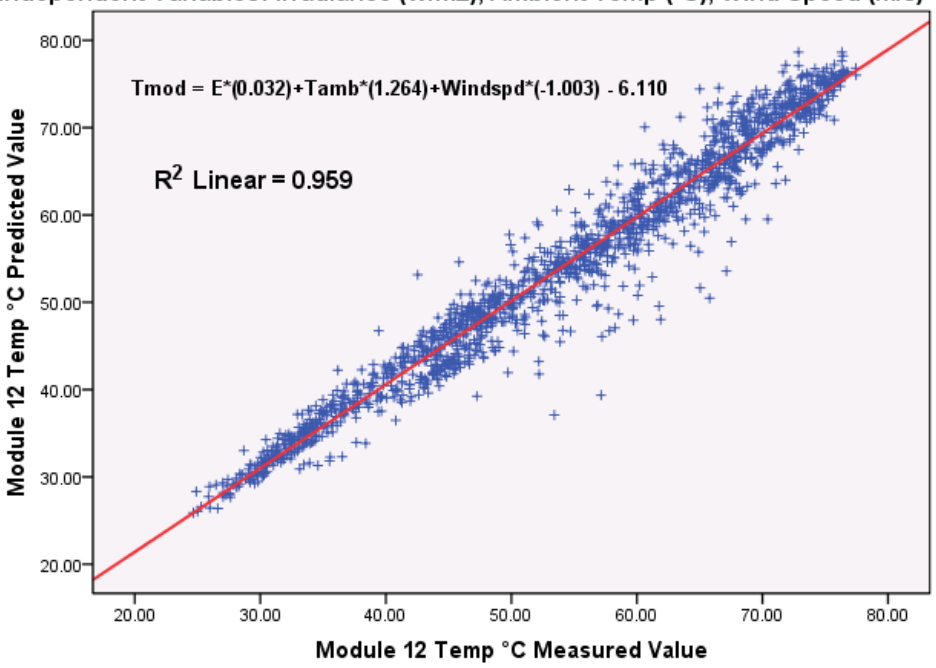

Array Average Temp °C Measured vs. Predicted Value

Independent Variables: Irradiance (W/m2), Ambient Temp (°C), Wind Speed (m/s)